LUT UNIVERSITY
LUT School of Energy Systems
LUT Mechanical Engineering

Juuso Pirttiniemi

DEVELOPMENT OF DESIGN PROCESS OF ROTARY KILN

20.9.2021

Examiner(s): Professor Timo Björk
M. Sc. (Tech.) Antti Taskinen

TIIVISTELMÄ

LUT-Yliopisto
LUT School of Energy Systems
LUT Kone

Juuso Pirttiniemi

Pyörivän uunin suunnitteluprosessin kehitys

Diplomityö

2021

79 sivua, 34 kuvaa, 18 taulukkoa ja 3 liitettä

Tarkastajat: Professori Timo Björk
DI Antti Taskinen

Hakusanat: meesauunin vaippa, skeleton-mallinnus, parametrinen 3D-malli, linjavirhe, tukikuormat

Tässä diplomityössä kehitetään parametrinen 3D-malli, joka toimii suunnittelutyökaluna meesauunin vaippalohkon suunnittelua varten. Uusi lohko tarvitaan kun vanhalle meesauunille tehdään huoltotoimenpide, jossa vaurioitunut osa uunin vaipasta vaihdetaan uuteen. Lisäksi työssä tutkitaan linjavirheen vaikutusta uunin tukikuormituksiin, mikä tarkoittaa vikatilaa, jossa uunin keskiakseli ei ole tukien suhteen suorassa.

Työssä perehdytään meesauunin rakenteeseen ja sen tehtävään osana valkolipeälaitosta ja kemikaalikiertoa. Lisäksi käydään läpi uunin eri vauriomuotoja, joita käytön aikana ilmenee ja on syynä huoltotoimenpiteille.

Suunnittelutyökalu kehitettiin soveltaen top-down skeleton mallinnusta, ja sen tavoitteena on mahdollistaa erilaisten vaippalohkojen suunnittelu tehokkaasti ja automatisoidusti. Malli sisältää vaipan komponentit, jotka ovat vaippalevyt, kannatusrengas, aluslaput ja kulutuspalat. Mallia ohjataan käyttöliittymällä, joka käyttäjän alkuvalintojen perusteella mudostaan oikean rakenneyhdistelmän 3D-malliin. Testikäytön tulosten perusteella, malli soveltuu meesauunin vaippalohkon suunnitteluun, ja tehostaa suunnitteluprosessia 2D-suunnitteluun nähden. Rakenteen mallin tehokkaan luomisen ja muokkaamisen lisäksi, 3D-malli mahdollistaa havainnollistavamman tuotteen esitysmuodon.

Linjavirheen vaikutusta tukikuormiin testattiin kolmetukisella ja viisitukisella uunilla, jotta erikokoisten uunien käyttäytyminen saatiin huomioon. Tulosten perusteella, linjavirheen vaikutus tukikuormiin on suhteessa voimakkaampaa viisitukisella uunilla. 5 mm suuruisella linjavirheellä havaittiin 10 prosentin kasvu tukikuormassa, mitä voidaan pitää kriittisenä kannatusrullien laakerien kestävyyden kannalta.

ABSTRACT

LUT University
LUT School of Energy Systems
LUT Mechanical Engineering

Juuso Pirttiniemi

Development of design process of rotary kiln

Master's thesis

2021

79 pages, 34 figures, 18 tables and 3 appendices

Examiners: Professor Timo Björk
M. Sc. (Tech.) Antti Taskinen

Keywords: lime kiln shell, skeleton-modelling, parametric 3D-model, axis misalignment, support forces

In this master's thesis, parametric 3D-model is developed that works as design tool for design of lime kiln shell section. New shell section is needed when service procedure is performed where damaged shell section from the old kiln is replaced with new one. In addition, this works studies the effect of axis misalignment on support loads, which means fault condition in which the central axis of the kiln is indirect with respect to the different supports.

The work introduces the lime kiln structure and its function as part of a white liquor plant and chemical recovery. Additionally, different forms of lime kiln damage are presented that occur during operation and could be a reason for maintenance.

The design tool is developed by utilizing top-down skeleton modelling, and its aim is to enable design of different shell section configurations effectively and automatically. The model includes main components of the shell that are shell plates, riding ring, filler bars and wear pieces. The model is controlled by user interface, that forms correct design into 3D-model based on user inputs. Based on test usage, the model can be utilized for designing of the lime kiln shell section, and it increases the efficiency of the process compared to 2D-design. Along with the flexible creation and modification of the design, 3D-model offers more illustrative presentation of the product.

The effect of axis misalignment on support loads is tested with three-support and five-support kilns for including the different behavior depending on kiln size. Based on the results, the effect of misalignment on support forces is higher with the five-support kiln. For a misalignment value of 5 mm, the increase on support forces is 10 percent, which can be considered critical for the durability of support roller bearings.

ACKNOWLEDGEMENTS

I would like to thank Andritz Oy for an interesting topic and an opportunity for this work. I am grateful for all the instructors involved in the work from Andritz, for their help during the thesis project. Special thanks to Patrik Blomqvist for his valuable and professional guidance related to this work and generally in the field of engineering. In addition, I would like to thank my supervisor from LUT University, Professor Timo Björk.

Finally, I want to thank my family for all the support during my studies and in life in general.

Juuso Pirttiniemi
Kotka, 20.9.2021

TABLE OF CONTENTS

TIIVISTELMÄ

ABSTRACT

ACKNOWLEDGEMENTS

TABLE OF CONTENTS

LIST OF SYMBOLS AND ABBREVIATIONS

1 INTRODUCTION 8

1.1 Research problem and research questions 8

1.2 Goals 9

1.3 Research methods and scope of the work 9

2 PROCESS DESCRIPTION 11

2.1 Chemical recovery 11

2.2 Lime reburning 13

2.3 Lime kiln shell 15

3 FORMS OF KILN SHELL DAMAGE THAT LEADS TO REPAIR WORK 19

3.1 Wearing 19

3.2 Shell ovality 20

3.3 Overheating 23

3.4 Deformations and axis misalignment 24

3.5 Fatigue cracking 26

4 PARAMETRIC SKELETON MODELLING AND MODEL-BASED DEFINITION 29

4.1 Top-down design 29

4.2 Model-based definition 32

5 PARAMETRIC 3D-MODEL FOR LIME KILN SHELL SECTION 36

5.1 Demands for the model 36

5.2 Parameters and user interface 37

5.3 Structure of the model 38

6 EFFECT OF SHELL AXIS MISALIGNMENT ON SUPPORT LOADS 45

6.1 Description of analysis 45

6.2 Ansys beam-model 45

7 RESULTS **51**

7.1 Quality of 3D-template model 51

7.2 The effect of axis misalignment 53

7.2.1 The effect on support forces for kilns 5,5 m x 165 m and 3,4 m x 90 m 53

7.2.2 The effect on bending stresses at support locations for kilns 5,5 m x 165 m and 3,4 m x 90 m 57

8 DISCUSSION **66**

8.1 Literature findings 66

8.2 Discussion of the functionality of lime kiln shell section 3D-model 67

8.3 Discussion of the effect of misalignment on support loads 68

9 CONCLUSIONS **72**

9.1 Further studies and future aspects 73

10 SUMMARY **75**

LIST OF REFERENCES **76**

APPENDIX

Appendix I: Model user interface, input data sheet

Appendix II: Result set for kiln 5,5 m x 165 m

Appendix III: Result set for kiln 3,4 m x 90 m

LIST OF SYMBOLS AND ABBREVIATIONS

ω_r	Relative ovality [%]
δ_v	Vertical deviation [mm]
δ_h	Horizontal deviation [mm]
D_n	Nominal inner diameter of kiln shell [mm]

2D	Two-dimensional
3D	Three dimensional
$CaCO_3$	Calcium carbonate
CaO	Calcium oxide
$Ca(OH)_2$	Calcium hydroxide
CAD	Computer aided design
CAM	Computer aided manufacturing
FAT	Fatigue class
MBD	Model-based definition
Na_2CO_3	Sodium carbonate
NaOH	Sodium hydroxide
NDT	Non-destructive method
WLP	White liquor plant

1 INTRODUCTION

Lime reburning is a process that relates in chemical circulation in pulp mill. Its main unit is lime kiln that converts calcium carbonate to calcium oxide which is used for creating white liquor that is auxiliary chemical in sulfate pulp cooking. The lime kiln is rotating drum made from bent steel plates, where the calcium carbonate is burned at high temperature.

In this thesis, mechanical design related to lime kiln maintenance process is developed, where section of the lime kiln is replaced. Different failures during usage of lime kiln can lead to maintenance procedure where the damaged section of the kiln is removed and replaced with new one. For increasing the design efficiency of new shell section components, parametric design tool is developed as part of this thesis. The work is made for Andritz Oy, which is one of the global leaders of supplying products and services in pulp and paper industry.

1.1 Research problem and research questions

Andritz service operation has need for making the lime kiln section change design process more efficient by creating a parametric three-dimensional (3D) model. The model would ease the development of required documents, such as manufacturing drawings, that are needed in shell section change projects. In current procedure, design work for kiln section is done by modifying drawing of the whole kiln. In other words, there is not tailored tool for designing section change and the documentation work basically starts from zero for a new project. The template model would reduce the design work time and allows to execute changes of lime kiln design standards centrally.

In addition to the 3D-model, structural analysis concerning the kiln loading behavior under axis misalignment state is deemed useful for gaining more knowledge about the phenomenon. During the operation, the position of the kiln supports can shift with respect with each other. That can be caused by sinking of the whole foundation when it also decreases the support position. Another reason can be the wear at contact surfaces between riding ring and support roller, which removes material from the surfaces and lowers the center of the shell at support. The axis misalignment causes several problems for the kiln.

The support force distribution among the different support changes from the initial state where they were designed. That may cause premature failures of the support components such as support rollers that faces the weight of the kiln. It also affects to the shell at support locations by the increased stresses, which for example affects to the refractory life by increased ovality. The increased information of the effect of misalignment for the support loads would be useful for the total knowledge of the kiln behavior which increases the possibility to predict forthcoming failures beforehand. Previous research problem can be formed in to following research questions:

- What are the main failure modes for the lime kiln that leads to repair work?
- How parametric 3D-model could be utilized for efficient design of lime kiln shell section?
    - How the model affects on the efficiency of the design work of lime kiln shell section?
- What is the effect of kiln axis misalignment on support forces and bending stresses at support locations?
    - How the effect of axis misalignment on support loads differs with kilns with different sizes?

1.2 Goals

The aim for this work is create parametric 3D-model template, that increases the efficiency of the design process of lime kiln section change maintenance process. The purpose of the template model is to have easily modifiable tool that helps at producing manufacturing documents of the new kiln section. The 3D-model also would be a step in moving from two-dimensional (2D) design to 3D-design. For the structural analysis part, goal is to find the effect of axis misalignment on support forces and bending stresses at support locations and compare them with different size of kilns. The information would be useful for understanding the effect of support position deviation and when it would be harmful for the kiln.

1.3 Research methods and scope of the work

Research methods that are used consist of literature review and practical development work. The literature review contains description of lime kiln and chemical recovery process in sulfate pulp production, failure modes that occurs at lime kiln, and theory of skeleton- and top-down design process. For the literature review strong references are preferred such as books and scientific articles related to the topic. For theory of the pulp production process and top-down design process there is scientific literature available which is used as reference. However, when the structure of the kiln is presented, Andritz's internal documents and reports are mainly used. That is because the information is then the latest and corresponds nowadays structures.

For the practical development part of the work, auxiliary tool for mechanical design process of lime kiln section change is developed. It is done by utilizing parametric skeleton-modelling using Autodesk Inventor software, which is computer aided design (CAD) software for 3D- modelling. The development work is done by utilizing knowledge of the Andritz experts in design. Modelling is made based of the different 0- models that the Andritz white liquor plant (WLP) have and following current design process and its tools in AutoCAD environment. For ensuring the quality of the 3D-model, it is tested with different scenarios. Structural analyzes are made by utilizing Ansys Workbench software, which is structural finite element analysis (FEA) software.

The scope of the work is defined in a way that the 3D-model includes a section of the shell that considers shell plates, riding rings, filler bars and wear pieces. The rest of the kiln shell is taken account as a reference. However, the model will be designed in way that it could be utilized into whole kiln shell parametric model in the future. For the structural analysis part, the effect of misalignment is studied from view of support forces and bending stresses at shell. The topic is studied for five-support and three-support kilns, which allows to compare the phenomenon for kilns of different sizes.

2 PROCESS DESCRIPTION

In this chapter, the process of chemical recovery and lime reburning is described in sulfate pulp production. In addition, structure and functionality of lime kiln is described as part of the process.

2.1 Chemical recovery

Chemicals that are used in sulfate pulping are expensive and for that reason, they are recovered and reused in sulfate pulp production. The purpose of chemical recovery in pulp plant is to transform black liquor back into white liquor which is the main cooking chemical. Schematic diagram of chemical recovery can be seen in figure 1.

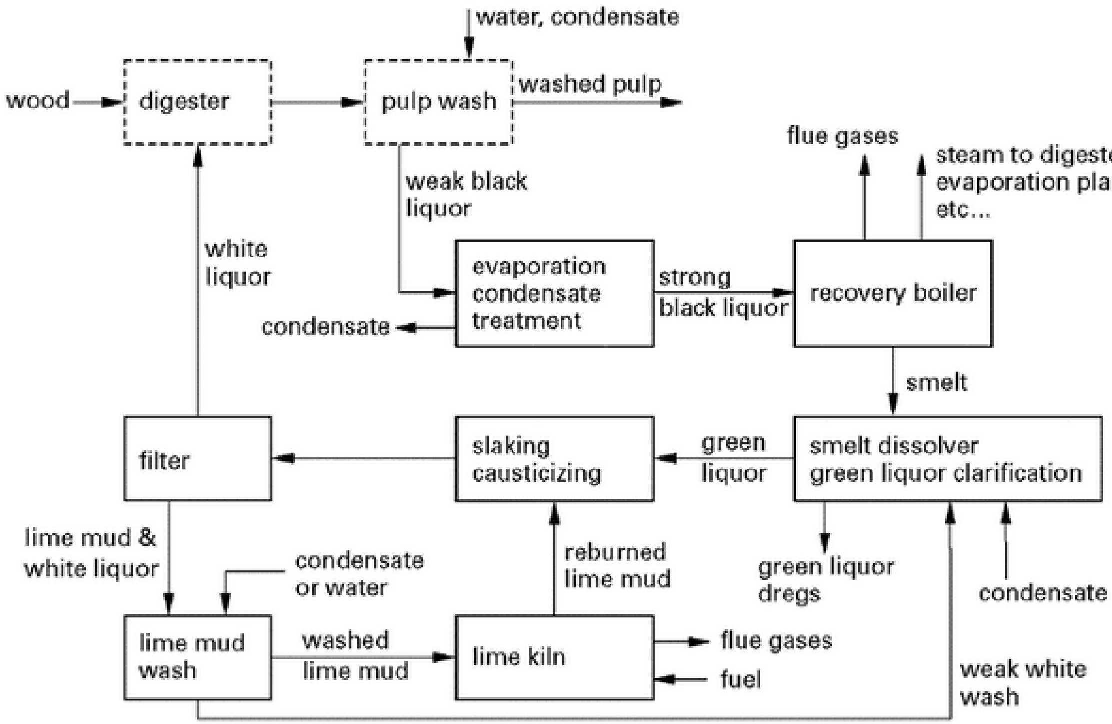

Figure 1. Chemical recovery process (Theliander 2009, p. 298).

The black liquor is formed when white liquor reacts with lignin in cooking process. The black liquor is lead from cooking to evaporation plant, where it is dried from water. After evaporation, the liquor is lead to the recovery boiler. Function of the recovery boiler is to release cooking chemicals, sulfur and sodium, from the black liquor by burning it. The chemical smelt from burning process is recovered and dissolved into weak wash which generates green liquor that is used in causticizing. Alongside of the chemical recovery, the burning of the black liquor generates heat energy that can be used as steam production and so on in electricity production. (KnowPulp 2021; Theliander 2009, pp. 314-315.)

In white liquor plant, the green liquor from the recovery boiler is turned into white liquor, which can be used in pulp cooking. Components of the white liquor plant are shown in figure 2.

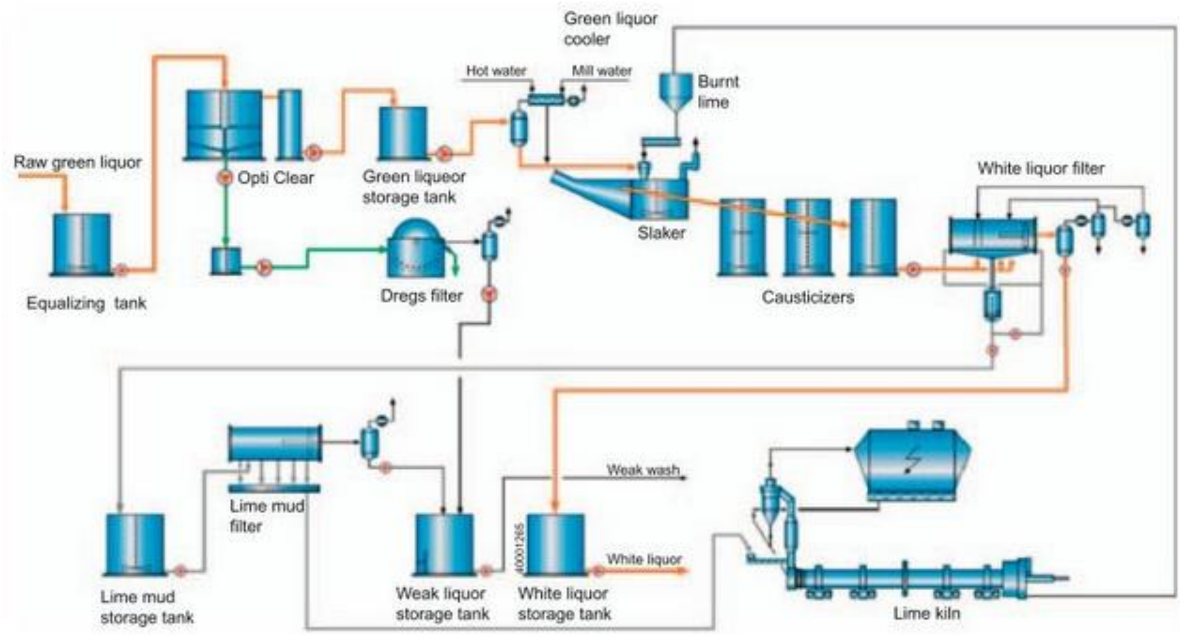

Figure 2. Components of white liquor plant (Bajpai 2016, p. 102).

The green liquor that is formed after recovery boiler is first separated from green liquor sludge by filtration or sedimentation process. Then the filtrated green liquor is transformed to the causticizing process where the creation of white liquor is occurred. Causticizing consists of two stages, slaking and causticizing. The reaction equation of slaking is shown in following equation. (KnowPulp 2021; Bajpai 2016, pp. 101-102.)

$$CaO + H_2O \rightarrow Ca(OH)_2 \tag{1}$$

In slaking, the green liquor is mixed with burned lime mud, calcium oxide (CaO). As can be seen in equation 1, the calcium oxide reacts to the water from green liquor and creates calcium hydroxide ($Ca(OH)_2$) When the calcium hydroxide is formed, the causticizing process begins. The reaction equation of causticizing is shown in following equation. (KnowPulp 2021; Bajpai 2016, pp. 101-102.)

$$Ca(OH)_2 + Na_2CO_3 \rightarrow 2\,NaOH + CaCO_3 \tag{2}$$

As can be seen from equation 2, the calcium hydroxide reacts with sodium carbonate (Na_2CO_3) from green liquor and creates sodium hydroxide ($NaOH$) known as white liquor. During the process, also calcium carbonate ($CaCO_3$) known as lime mud is formed. The white liquor and lime mud are then separated by white liquor filter. After filtration, the white liquor is available for sulfate cooking. The lime mud is lead to the lime reburning, where it will be transformed back to calcium oxide which is used again in causticizing. Although, the lime mud from white liquor filter contains weak white liquor, so it is washed and separated before lime kiln. Particular process is occurring in lime mud filter. The processes of slaking, causticizing, lime mud wash and lime reburning is also known as calcium cycle. That is because the calcium participates in these processes in three different forms, calcium carbonate, calcium oxide and calcium hydroxide. (KnowPulp 2021; Bajpai 2016, p. 102.)

2.2 Lime reburning

As mentioned previously, lime reburning is part of the calcium cycle, where the calcium carbonate, lime mud, is transformed back to calcium oxide. The calcium oxide is auxiliary chemical that is used in causticizing process, where green liquor is transformed into white liquor. The aim for the lime reburning is to reuse and cycle the calcium and hence minimize bought calcium oxide. For creating this reaction where calcium carbonate transforms to calcium oxide, calcination temperature must be achieved which is above 850 °C. It is produced in rotary kiln where the lime mud is burned in about 1100 °C for ensuring fast enough reaction speed. The lime reburning unit processes can be seen in figure 3. Lime mud burning involve the following steps:

- Lime mud feeding
- Lime mud drying
- Heating the lime mud for reaction temperature

- Calcination of lime mud
- Handling of reburned lime mud.

(Bajpai 2016, p. 131; KnowPulp 2021.)

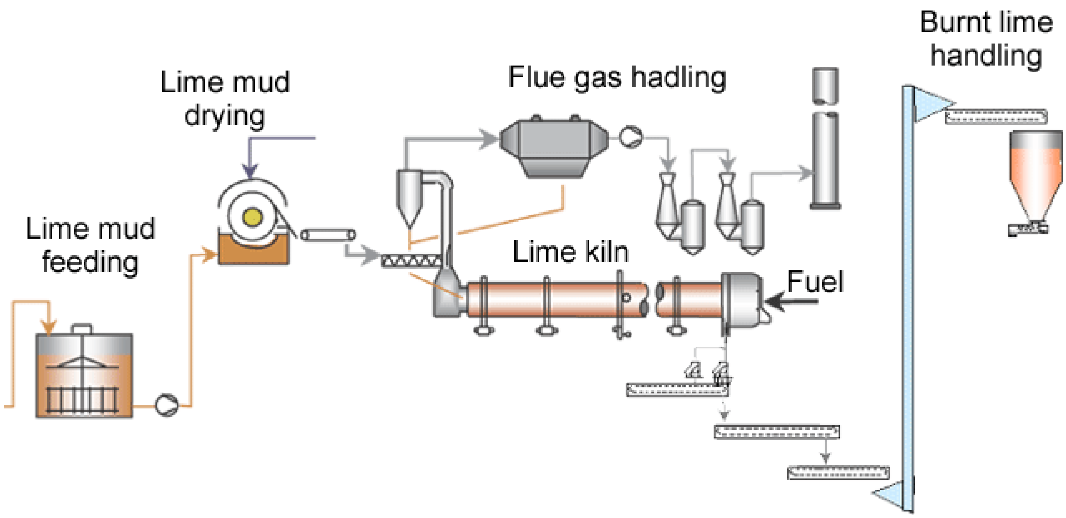

Figure 3. Lime reburning unit processes (KnowPulp 2021).

Before feeding lime mud into lime kiln, it is washed and dried at lime mud filter, where its dry content level is increases typically at 75-80% after filtering. The final drying is occurring at kilns dryer where it dried for almost 100% dry content level. The dryer is vertical duct that locates at the feed end of the kiln. The mud is conducted along the duct and with help of the hot flue gasses from the kiln, it is dried almost completely. The flue gasses are then separated from the dried mud in cyclone, which leads the lime mud into the feed end of the kiln. (KnowPulp 2021.)

Due to the lime kiln rotation and small incline of the shell, the fed lime mud starts to roll along the kiln. The burn end locates at the low end of the kiln, so the flue gasses are flowing against the lime mud movement. For that reason, while lime mud is flowing through the kiln, its temperature rises until it finally reaches the burning zone where the temperature is enough for calcination reaction. The calcination is chemical reaction that occurs according to following equation. (Bajpai 2016, p. 131.)

$$CaCO_3 \leftrightarrow CaO + CO_2 \tag{3}$$

In calcination reaction (equation 3), the calcium carbonate transforms to calcium oxide and carbon dioxide (CO_2). The burned lime has high temperature, so it has to be cooled before feeding forward. The cooling is done by heat exchange where heat energy from the burned lime is transformed to the cool secondary air that is sucked inside kiln. In modern kilns, the cooling is executed with sector cooler that is implemented in burn end of the kiln. It consists of two nested cylinders that are concentric with the kiln shell. Between the cylinders, there are plates that divides the area between into sectors. The burned lime drops from the kiln to the cooler and flows to the lime conveyor. (Theliander 2009, p. 356; KnowPulp 2021.)

2.3 Lime kiln shell

The lime kiln is rotary kiln where the lime mud is burned as presented previously. It has slight incline, typically 2.5%, and slow rotation speed (1-2 rounds per minute), which enables the lime mud flow. The kiln shell consists of bended steel plates that are welded together and supported by foundations where support rollers and riding rings allows the kiln to rotate. The number of supports is determined based on the size of the shell, in which Andritz has variation in diameter from 2.4 meters to 5.5 meters and the length from dozens of meters to even couple of hundred of meters. Because of the high temperatures that are needed for calcination, the inside of the shell is lined with refractory masonry that protects the steel shell from heat. The heat effect is higher at the fire end because of burner flame, so the refractory must be thicker there than in other parts of the kiln. The lime kiln is shown in figure 4. (Koskinen & Mussalo 2006, p. 6; Andritz Oy 2019, pp. 56-58.)

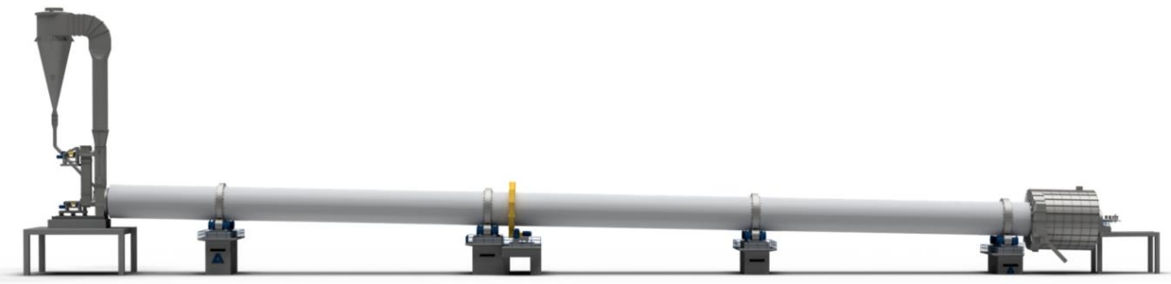

Figure 4. Lime kiln (Andritz recovery and power 2020, p. 4).

The main components of lime kiln shell are shown in figure 5. Shell plates have different thicknesses through the length of the kiln. Because of the thicker refractory lining at fire end and the weight of the cooler, the fire end is the most loaded part of the kiln. That is why overall, the shell thickness increases towards the fire end. However, the thickest shell plates are at the support locations because of the bending moment peaks of the shell. Between the thick and thin shell there can be used one or two different mid thicknesses that are called flankers. (Koskinen & Mussalo 2006, pp. 6-7; Andritz Oy 2020b, p.5.)

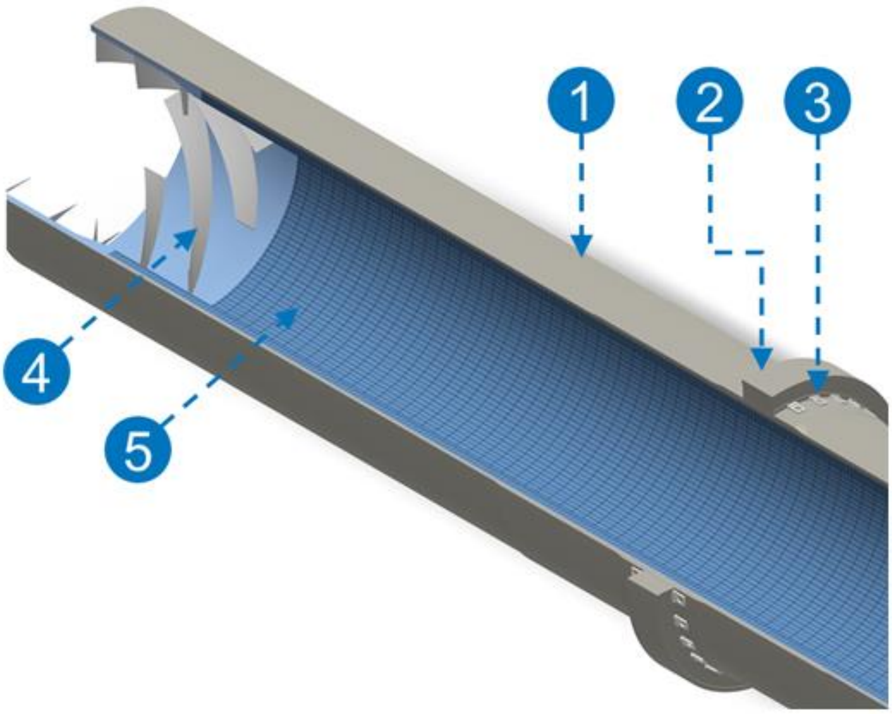

Figure 5. Components of lime kiln shell: 1. Lime kiln shell 2. Riding ring 3. Riding ring wear pieces 4. Feed flights 5. Refractory lining (Andritz Oy 2020a, p. 15).

The shell of the kiln is connected to the support rollers by riding rings that supports the rotation motion of the kiln. Riding ring is installed at the surface of the shell "freely", meaning that it is not fastened rigidly to the shell. There is determined to be 5 mm clearance between the riding ring inner diameter and shell outer diameter, which is illustrated in figure 6. The clearance is determined because of the heat expansion during usage. The temperature rises faster at the thinner shell, so the thermal expansion is larger. That way if the fit is too tight between shell and ring, the expansion of the shell would be restricted by the ring. That would cause deformations to the shell and the refractory lining breaks at that location. The clearance is dimensioned in a way that when the kiln warms, shell circumference grows for closer match to tire. Although, it is desirable that the shell doesn't quite catch the ring inner diameter, so damage can be avoided. Because the ring is positioned freely around the shell, the axial movement needs to be restricted for avoiding the shifting along the length of the shell. That is done by wear pieces that are welded to the shell, or filler bars, for both sides of the ring. (Koskinen & Mussalo 2006, pp. 28-31; Gebhart 1995, p. 3.)

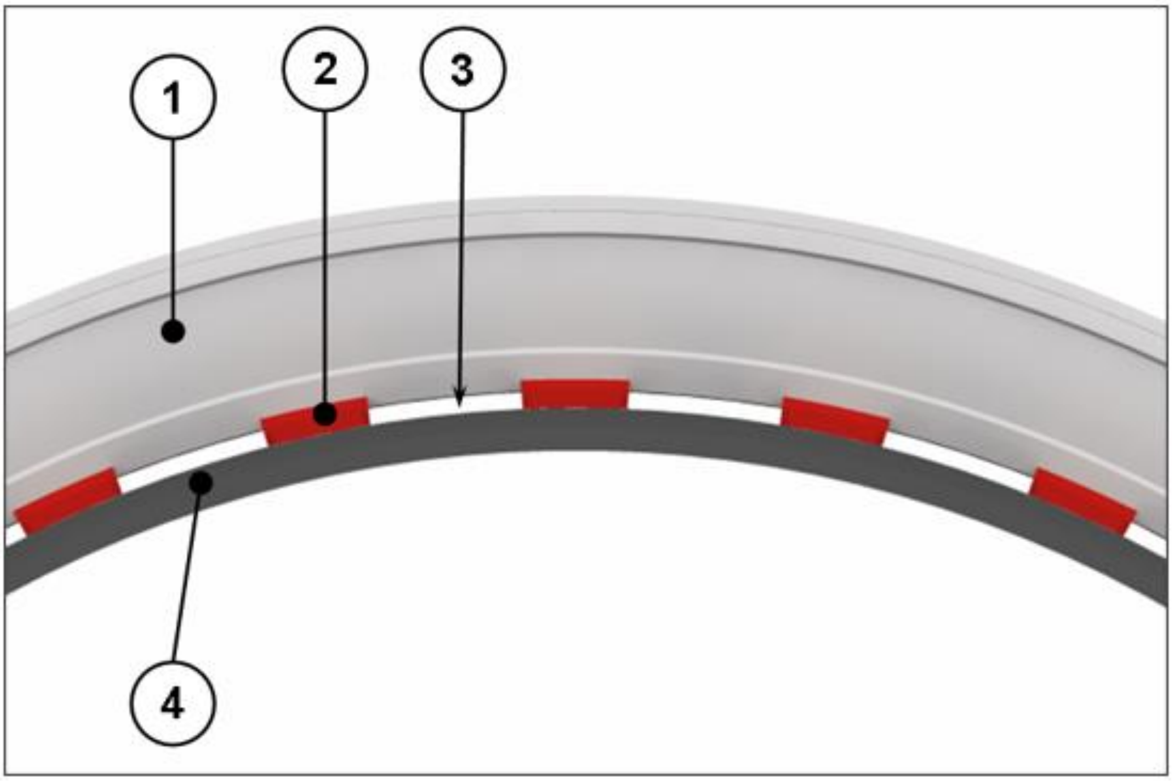

Figure 6. Riding ring area: 1. Riding ring 2. Riding ring wear pieces 3. Clearance between riding ring and kiln shell 4. Kiln shell (Andritz Oy 2020b, p. 14).

The whole kiln is supported axially by thrust roller (figure 7). Thrust roller is located at the same pier as the driving mechanism which rotates the kiln. It controls the movement of the kiln axially. Depending on the kiln, there can be thrust bearings both side of the guiding riding ring, which has machined contact angle corresponding to the thrust bearing contact angle. The guiding riding ring locates only at the driving support where the thrust bearing is. (Andritz Oy 2018, p. 17.)

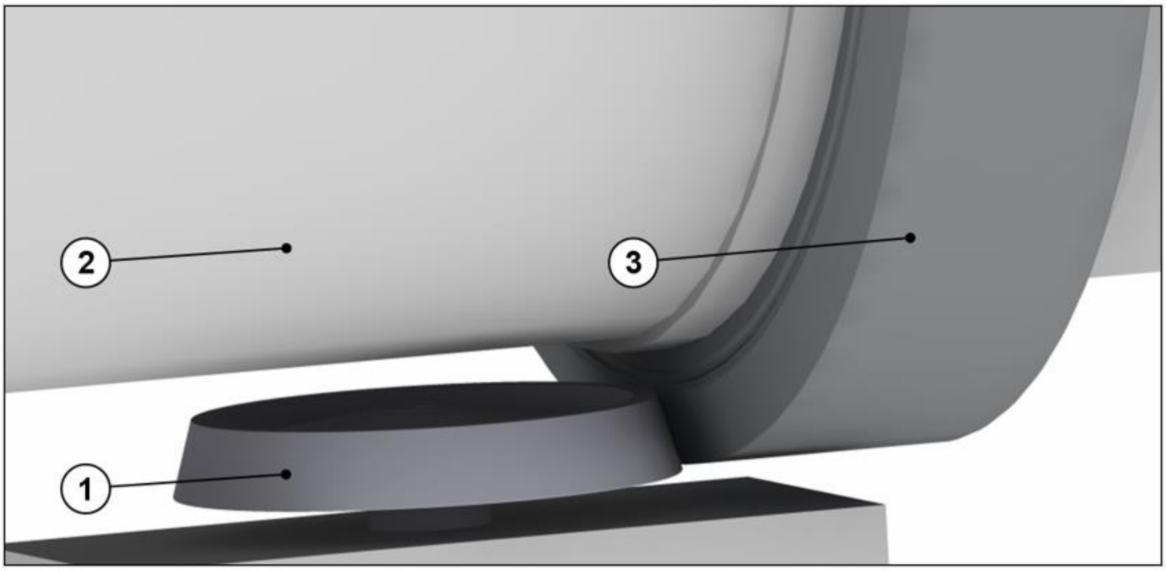

Figure 7. Thrust roller location: 1. Thrust roller 2. Kiln shell 3. Guiding riding ring (Andritz Oy 2018, p. 16).

3 FORMS OF KILN SHELL DAMAGE THAT LEADS TO REPAIR WORK

In this chapter, different failure modes of the kiln shell that can lead to section change are presented. The lime kiln is large and heavy machine so different kinds of failures may occur, and the important ones are collected to this chapter. The repair works can be expensive for the owner of the kiln, especially if the production must be shut suddenly because of the failure, and the lime must be bought. That is why the constant maintenance and regular measurements are in key role for preventing failures to occur unexpectedly.

3.1 Wearing

Between riding ring and kiln shell there is designed to be clearance for thermal expansion as presented in chapter 2.3. The clearance causes phenomenon that the ring falls behind from the rotation speed of the shell. That means that there is little sliding occurring between riding ring and shell. This relative movement of shell and riding ring is called creep that causes wear for the surfaces which leads to increase of the clearance. From the figure 8 can be seen the effect of wear between ring and shell. Increased clearance causes more problems, for example increased ovality. Little creep is however an indicator that the gap between ring and shell is not too tight and it is functioning properly. The wear is restrained by lubricating the contact between ring and shell where it prevents the mechanical wear but doesn’t increase the creep too much. A proper lubrication between ring and shell increases durability of shell, tire and refractory significantly. However, the lubrication can’t have access between support roller and ring contact. That can cause the support roller to stop, which damage the contact surfaces. (Gebhart 1995, pp. 3-4); Andritz Oy 2020b, p. 12.)

Figure 8. Example of increased clearance between shell and riding ring due to wear.

The movement of ring causes sliding between wear pieces and riding ring. The creep causes circumferential slipping and the radial clearance between ring and shell causes radial slipping. By lubricating the contact surfaces, the breakage of the components is tried to avoid. It is important because the particles that could loosen from the surfaces may reach the contact between ring and shell, which could lead to severe damage of shell. Also, the wear pieces themselves can be damaged and won’t be able to restrict the movement of riding ring. Wearing also occurs between riding ring and support roller. The roller surface is wider than the ring, so the pressure causes uneven wear that leads to irregular surface profile. As the wear increases, different problems occur such as vibrations, increased power consumption, bearing damage, decrease of kiln control and even the ring could crack. For avoiding those failures, the contact surfaces are machined regularly. That way the contact can be remained even, and repair work could be avoided. (Gebhart 1995, pp. 3-4; FLSmidth 2015, pp. 2-3.)

3.2 Shell ovality

Ovality, known as radial bending of the kiln is one of the typical reasons for kiln shell repair work. Ovality means elastic distortion of the shell during dynamic rotation caused by gravity force. It occurs the most at the support locations, where the shell is supported by rollers and ring. Gravity causes the top of the shell to flex downwards for each revolution and it loses its roundness. Respectively, the shell pushes in at the support roller locations, where the support forces are occurring. The ovality is severe problem for the refractory lining, because when the roundness of the shell changes, the refractory bricks can loosen, or even fall down. If the refractory lining is functioning improperly, the steel shell could be exposed for too high temperatures which can cause deformations or even failure. The refractory lining failure leads typically to repair work where the shell section is changed. The ovality of the shell and the destruction mechanism of the refractory lining are shown in figure 9. (Sengupta 2020, pp. 341-345.)

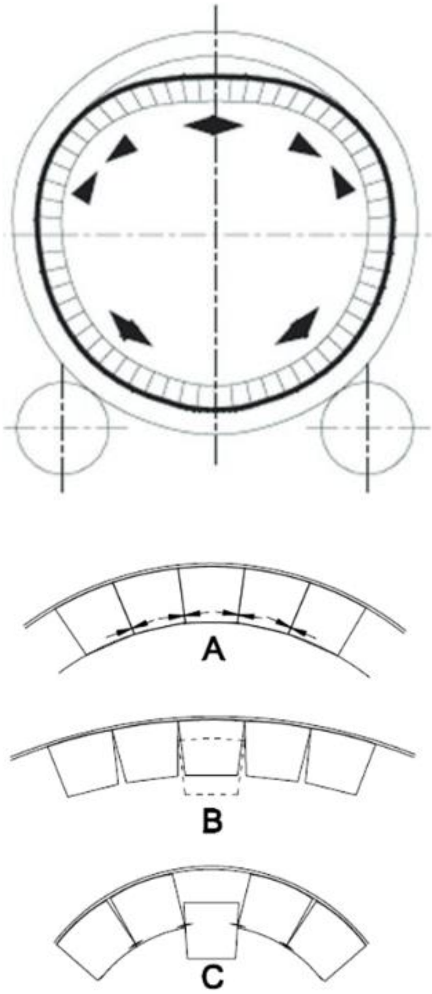

Figure 9. Ovality of the kiln shell and its effect on brick lining (Sengupta 2020, pp. 343-345).

The ovality is presented in percent unit, and it means the relation of the deviation of the shell to the theoretical inner diameter of the shell. One method of calculating relative ovality is shown on following equation.

$$\omega_r = \frac{100(\delta_v + \delta_h)}{D_n} \% \tag{4}$$

In equation 4, ω_r is relative ovality, δ_v is vertical deviation, δ_h is horizontal deviation and D_n is nominal inner diameter of kiln shell (Sengupta, 2020, p. 341). Ovality itself is always present, but too high values cause problems with the refractory. Increase of ovality is caused by the clearance between shell and riding ring. The riding ring is much stiffer than the shell locally, so it is maintaining the roundness and simultaneously maintains the roundness of the shell and refractory. When the clearance increases, the supporting effect of the ring decreases, and the shell is not anymore supported at the top and it flexes downwards. However, there must be clearance between ring and shell in order for proper function of the kiln after thermal expansion, as mentioned previously. For that reason, the ovality value should not be too small, because that indicates that the clearance between ring and shell is disappeared and the refractory is exposed for damage. For controlling the clearance, tire pads or filler bars, are installed between ring and shell. Then the wearing occurs for the shim plates instead of shell, and they can be replaced when the clearance gets too high. The magnitude of ovality is depended on many factors such as support angle of the rollers, clearance of riding ring and stiffnesses of shell and riding ring. Therefore, measurements are the most accuracy way for monitoring the ovality of the shell, because lot of different factors makes estimation by calculations difficult and complex. Some recommendations for the ovality values can be seen in figure 10, but the durability of the refractory is depended on its type. There can be seen that the critical ovality percent is higher when the kiln size increases. (TomTom-Tools GmbH 2018a, p. 15; Gebhart 1995, p. 3.)

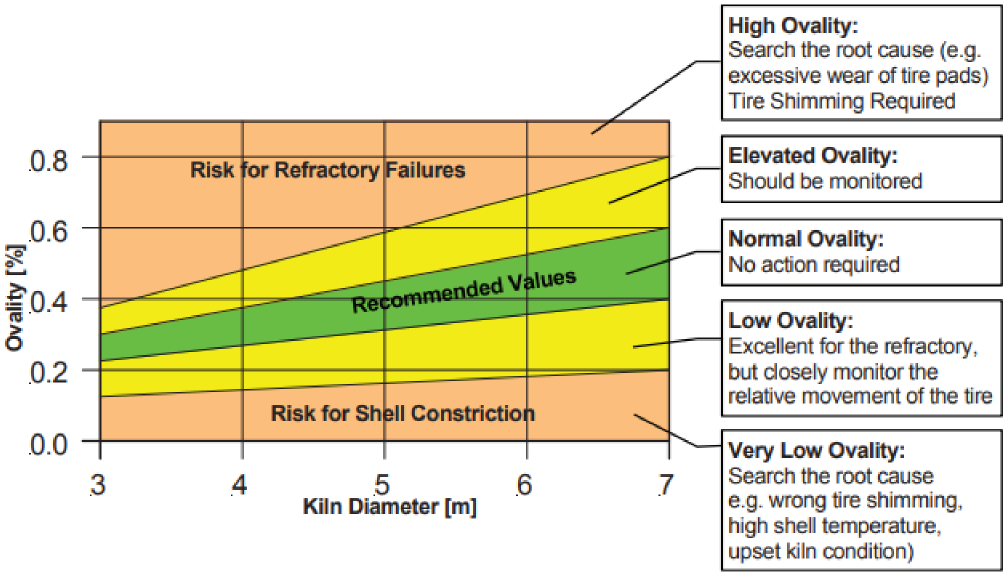

Figure 10. Typical ovality value limits (TomTom-Tools GmbH 2018a, p. 15).

3.3 Overheating

The refractory lining inside kiln shell can be damaged severely because of the overheating. Too high temperatures can be caused by thermal imbalance where the thermal input is too high in comparison to feed and exit rate of the kiln. The main parameters for controlling thermal imbalance for operator are fuel burning rate and rotation speed of the kiln. However, the operator is not able to control the material flow inside the kiln and that can cause overheating locally. For example, ring formation can cause thermal peak locally at the refractory. Also, the variation of lime mud and fuel properties can cause uneven wear of the coating, which could be difficult to estimate. If the refractory lining is damaged, the steel shell is not covered from the heat and so-called hot spots are developed. One example of visible hot spot can be seen in figure 11. Steel loses its mechanical properties in high temperatures, which are occurring inside the kiln, so there is a high risk for deformations of shell or even shell failure, if the insulation is inappropriate. If the hot spots are occurred, the shutdown of the kiln is started for the kiln to cool down. However, the kiln rotation should not be stopped, because then heat effect becomes very high locally. That may cause for example more refractory lining damage and shell distortion. Also, excessive heat expansion of the shell can occur, which causes extra loadings at the ring area when the clearance is reached. There is still possibility to continue operation, if the hot spots are detected and their temperatures are under critical limit. In that case, those areas require external cooling for restraining the temperature rise. (Sengupta 2020, pp. 337-340; Andritz Oy 2020b, pp. 9-13.)

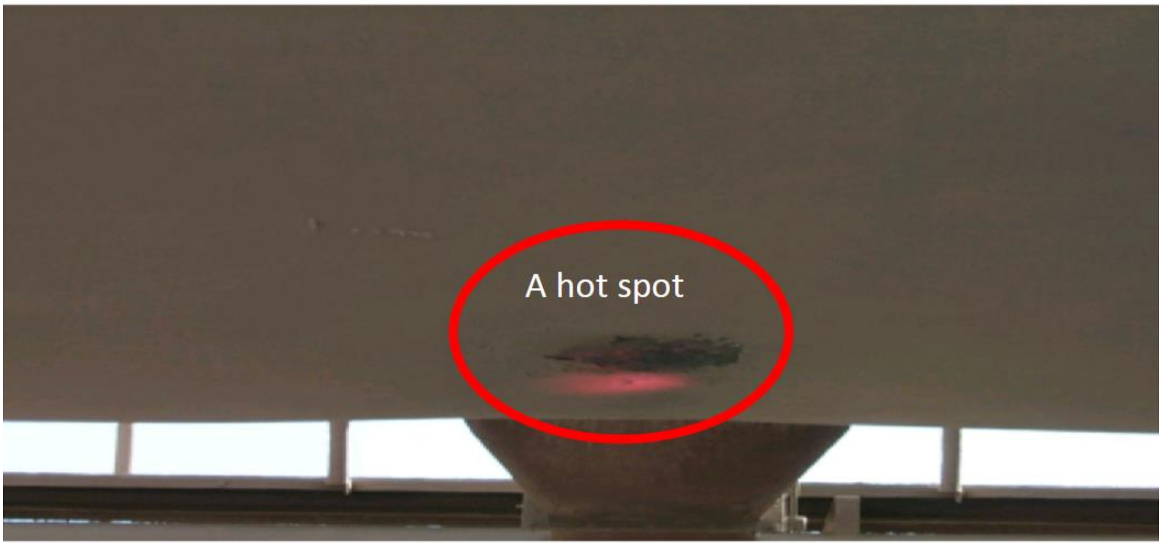

Figure 11. Visible shell hot spot (Janati 2020, p. 4).

3.4 Deformations and axis misalignment

Because of the kiln heavy weight and long structure, there is inevitably deflections between the supports. For that reason, the kiln is designed in a way that the deformations are minimized, and the rotations are zero at the support locations, so that won't affect on the functionality of the kiln. However, in some situations, loadings may get too high and deformations for the shell can occur. That can lead to "crank-shaft" behavior for the shell (figure 12), where rotational axis is not anymore at the geometrical center of the shell. That causes problems at the supports, because the load distribution is not anymore how it was designed. If the shell is bent, it develops situations where some supports have less loading and some more. That causes peaks of loadings at the support rollers, which could eventually lead to shaft failure for example. Along with the support forces, ovality and bending stress of the shell at support area increases. Also, the "crank" causes increase of cyclic loadings, which accelerates fatigue phenomena at the structure. For example, the fatigue affects at the base material for the roller shafts, but also the welds of the shell, especially the welds of side guide pieces, are critical for fatigue perspective. The crank is usually caused by damage of the refractory, which exposes the shell for the heat that deforms the steel shell. Another reason can be that the kiln is shut down too rapidly (when it has still high temperature) and thermal affection combined to gravity force deforms the kiln shell plastically. For that reason, the kiln should not be still for more than 10 minutes when it is hot. (Tom-Tom Tools GmbH 2018b, p. 16; Wisner 2020.)

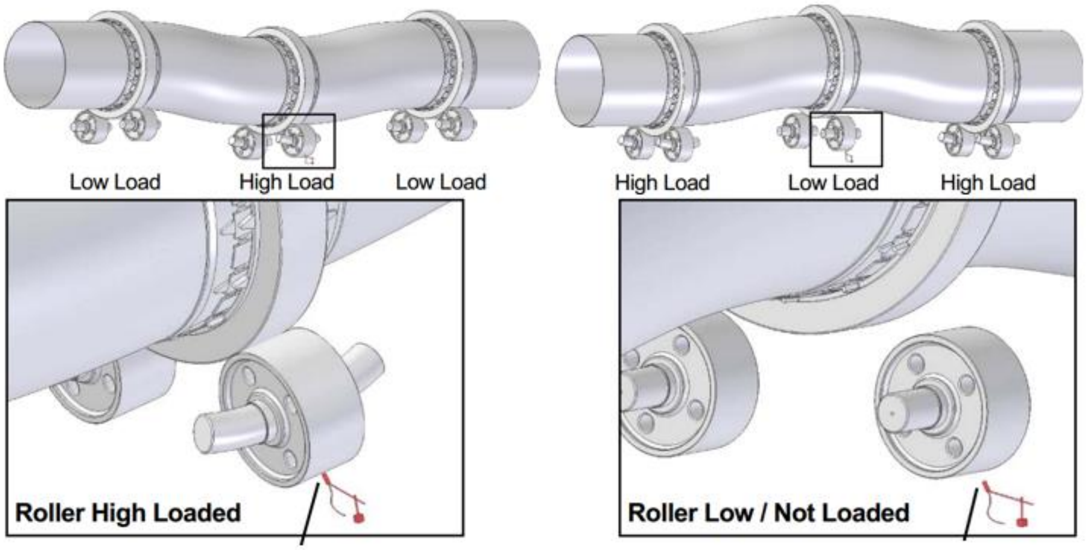

Figure 12. Crank of the shell (Tom-Tom Tools GmbH 2018b, p. 16).

Another state that causes problems at supports is the misalignment of the kiln axis. The misalignment can be critical state from a view of endurability because it increases the possibility of premature failure of components. It is problem for kilns that have three or more supports. The misalignment means that the kiln axis is not in a straight line along the supports, and the support load distribution becomes incorrect among different supports. Basically, that means that some of the supports are in different position as they were designed which creates the indirectness of the axis. Like the shell crank, the misalignment increases support forces that effects on bearing loads which can lead to bearing failure. When the support forces increase, the wear and ovality of the shell rises which affects to the refractory lining. It also changes the bending stresses of the shell at support locations which could lead to problems as time passes. In addition, the power consumption increases when the motor has more resistance. The phenomenon is different depending on if one of the supports is elevated or sunken. If the support is at lower position, the loadings of the pier are transforming for the adjacent piers. On the other hand, if the support is at higher position, the elevated support receives loadings from the other supports. The misalignment can be a reason for subsidence of the whole pier, which causes the kiln shell deviation. Another cause for a misalignment is the wear of ring at supports, which lowers the center of the shell also. If the wear is uneven between supports, the misalignment occurs which again accelerates the wear itself. Also, incorrect alignment at installation or after repair work could be a reason for indirect shell axis. (TomTom-Tools GmbH 2018c, p. 1; Yougang et al. 2008, p. 319.)

3.5 Fatigue cracking

Cracking of the shell occurs usually at the support location where the loadings are the highest. These cracks are caused by the welds of the filler bar plates or side guide pieces, that are welded directly to the shell. One example of detail that is directly welded to the shell is shown in figure 13.

Figure 13. Example of components welded directly to the shell.

The rotational movement of the kiln creates cyclic loading for the welds, which makes them prone to fatigue cracks. The developed crack grows from the attachment weld along the shell surface. Example of shell cracks in longitudinal direction can be seen in figure 14. At worst, the crack reaches the circumferential weld and starts to grow along it. That may lead to failure of the circumferential weld that could cause the shell to rupture. For slowing the growth of the fatigue cracks, repair welds are made as a maintenance procedure, where the crack path is welded on. However, that doesn't stop the growth entirely, and eventually the shell must be changed.

Figure 14. Example of shell cracks (side guide pieces removed)

The reason that the crack occurs at the attachment welds is because of the weld type and geometry. The welds cannot be through welded so there is always initial crack occurring. Also, the stiffness of the attachment plates differs from the shell, which creates additional stress peaks for the welds as the kiln rotates. The criticality of the attachment welds can be also verified basically with fatigue classes (FAT). Compared to other welds at the support area, which are circumferential and longitudinal welds of the shell, the attachment welds have lower fatigue class than the others. Fatigue class means characteristic fatigue strength for the welded detail in megapascals at 2 million cycles (SFS-EN 1993-1-9 2008, p. 9). The longitudinal and circumferential welds of shell are fully penetrated double-sided welds and with the welding class B, they are tested with nondestructive testing (NDT) methods. According to Eurocode 3 and International institute of welding (IIW), the fatigue class for circumferential welds, that are transverse butt welds are between 80-112, and for the longitudinal welds 125, if automatic welding process is used (Hobbacher 2008, pp. 48-51;

SFS-EN 1993-1-9 2008, pp. 22-25). When the attachment welds have FAT-class around 50-63, it verifies that they are the most critical location for fatigue perspective (Hobbacher 2008, p. 64). Those fatigue classes are not valid directly because the designs are differing depending on the kiln age and manufacturer. However, they can be used for noticing the difference between attachment welds and through welded butt welds in fatigue perspective.

4 PARAMETRIC SKELETON MODELLING AND MODEL-BASED DEFINITION

In this chapter, theories of different design and modelling methods are presented, which are utilized for the development of parametric 3D-model of the lime kiln shell section. Dealt topics are related to parametric design with top-down method. In addition, a theory of a technology called model-based definition is introduced.

4.1 Top-down design

Generally, there are two different design methods for 3D-CAD design, bottom-up design and top-down design. Traditional (bottom-up) design procedure starts the design with single components and then combine them into assemblies with constrains. In this method, the single components don't have any other relation than the upper-level assemblies where they are imported. Modifying the design in bottom-up design for large assemblies can be laborious, because the changes need to be made for each part separately and the relationships between parts might have to be rearranged. In top-down design, the individual components have relation for top level shared parameter that controls the component path. The common parameter can be for example variable or geometry. With this method, the changes are made in top level and the information is shared for every linked component. This way changes can be made without modifying every component individually. It is common to create a master model, where the subassemblies and components are linked. This kind of modelling is called skeleton-modelling. Skeleton-model can be used for creating the geometries of individual components and positioning them into correct location in coordinate system. That way the constraints between components can be avoided. Even if the top-down modelling is used, usually also bottom-up modelled components are included. For example, standard parts that are used in several different designs, are made with bottom-up method. (Pere 2016, p. 30; Chu et al. 2016, pp. 1-2.)

3D-model templates are used for rapid variant designing when the designed products are same or similar which each other. Assembly design template is created in a way that the components of the assembly automatically maintain the original relationships to each other even if the overall design changes. The templates could be then reused for different variations and that way they are efficient method of handling for example product series design. Utilizing parametric design method for the model templates, designed products are able to have adaptability efficiently. The template can be controlled by key parameters that have effect on the structure of the design, for example size of the product. Parametric modelling means that besides the structural parameters that controls the design of the product, other parameters are used that control how the structural parameters are determined. In other words, the parameters have relationships with each other. That means by modifying certain key parameters, for example size of the product, the structural parameters and component properties modify automatically. Adding parameter modelling as part of an engineering process, leads reduction of time that is spend on applying modifications on each feature when overall design is changed. Even though applying parametricity into 3D-models uses more time and resources initially for the development work, the power of managing changes of the designs is the benefit that makes it worth it. (Jiao 2014, pp. 289-290; Autodesk 2020, pp. 4-5.)

An example case where top-down skeleton design method is utilized, is presented next for more illustration of the technique. Chen et al. (2012, p. 1043) presents in their research an example of multi-level assembly that is designed by top-down design method. They designed a sample of engine starting by overall function and shape skeleton, and then proceeded for more detailed geometry and design. The engine consists of six components, four parts and two sub- assemblies. The structural diagram of the assembly is shown in figure 15.

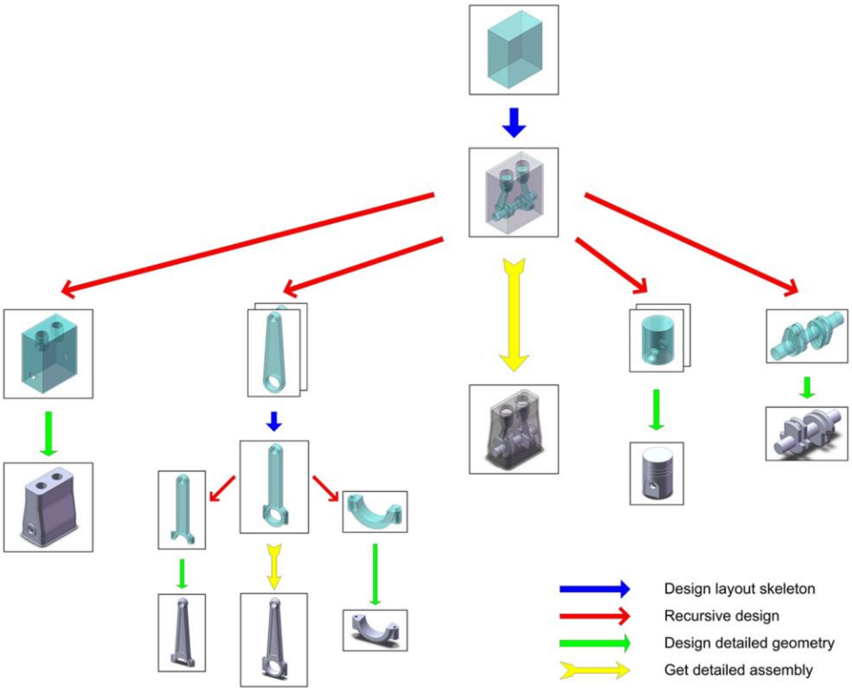

Figure 15. Top-down assembly design process for engine (Chen et al. 2012, p. 1044).

From the figure can be seen how different the skeleton models are controlling the whole structure. The shape skeleton evolves to layout skeleton, from which the shape skeletons of components are created. The shape skeletons are coarse, and the detailed geometries are formed in the part creation phase. Finally, the different parts are combined into engine assembly. The structure model shows in general level the idea of top-down design, and how the different components are linked with each other. In this kind of design, the whole assembly is controlled by the layout skeleton and the modifications of the design are made in that level. The modification example with parameters is shown in figure 16. From the figure can be seen that the layout skeleton of the engine can be used for controlling the whole assembly. The links between different components ensures that the model changes correctly if the parameters of the layout skeleton is modified. (Chen et al. 2012, pp. 1043-1045.)

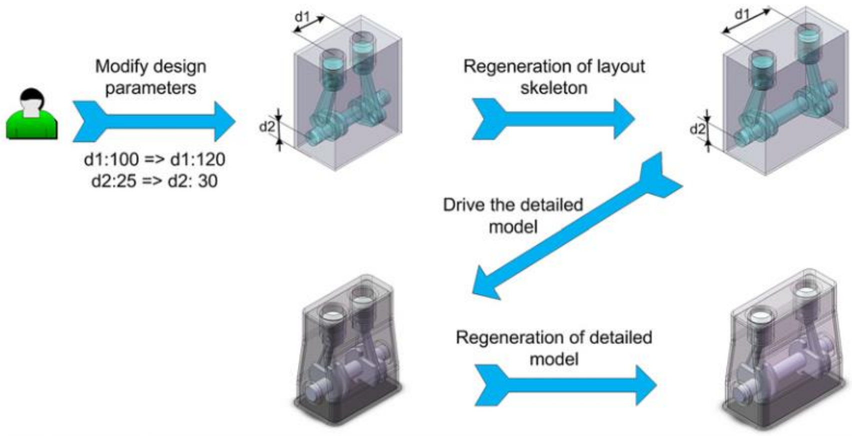

Figure 16. The propagation of change on modification of parameters in the layout skeleton of engine (Chen et al. 2012, p. 1046).

4.2 Model-based definition

Model based definition (MBD) means technology, where the 3D-model includes all the detailed information of the product for downstream users. It means the drawing annotations are integrated for the 3D-model, which reduces the need of traditional 2D-engineering drawings. That way the source of data is concentrated into one type of file, instead of separate model file and drawing file. By including the drawing annotations and geometrical tolerances for the model, for example the implementation in computer aided manufacturing (CAM) machining processes is more efficient, which can be time saving. An example of MBD- model can be seen in figure 17. (Quintana et al. 2010, p. 498; Thilo 2019.)

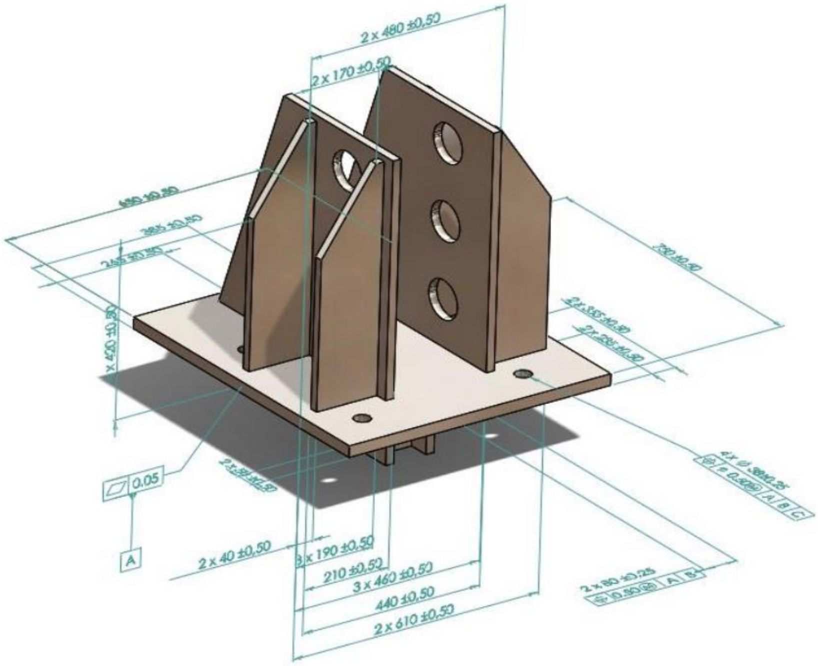

Figure 17. Example of model-based dimensions and tolerances implementation in 3D-model (Varitis, Rinos & Kostis 2020, p. 3).

Along with the manufacturing aspects, the model-based definition introduces other benefits for its use. In traditional design practice, for the same part there is two different design definitions by form of 3D-model and drawing. The MBD dataset generates only one source for the design data and by that reduces the time and database with need of controlling only one file. Another aspect relates to downstream user understanding of the design. Perception of the structure from 2D-drawing requires time and training but with 3D-geometry, also non-designer users can easier understand the design of the product. In addition, there might be cases where the 2D-projections won't be able to describe the structure completely correct. With the 3D-presentation, the user can for example rotate and zoom the design, which helps with the perception and the scope for interpretation is left to a lesser role. (Quintana et al. 2010, pp. 498-499; Varitis et al. 2020, pp. 3-4.)

However, there is still several limitations for fully adapting the MBD- system and eliminating 2D-drawings. The accessibility for the CAD-software would need to be ensured for wide section of users, because the files are only readable in 3D-environments. Although, overcoming this problem lightweight formats are used presentation of the MBD-dataset. For example, one of the used file types is 3D-pdf (figure 18), which includes view of the product geometry or assembly and important information for downstream users like revisions or physical properties for instance. Besides the needed hardware improvements, also several personnel would require 3D-softvare manipulation skills. Model-based definition differs a lot from the traditional 2D-drawings. It needs more upfront work compared to traditional method for achieving bigger impact on downstream users. Also, the change is usually difficult to accept, especially if the current method is working. That is one reason which slows down the transformation to MBD in companies. (Varitis et al. 2020, pp. 4-6; Nguyen 2021.)

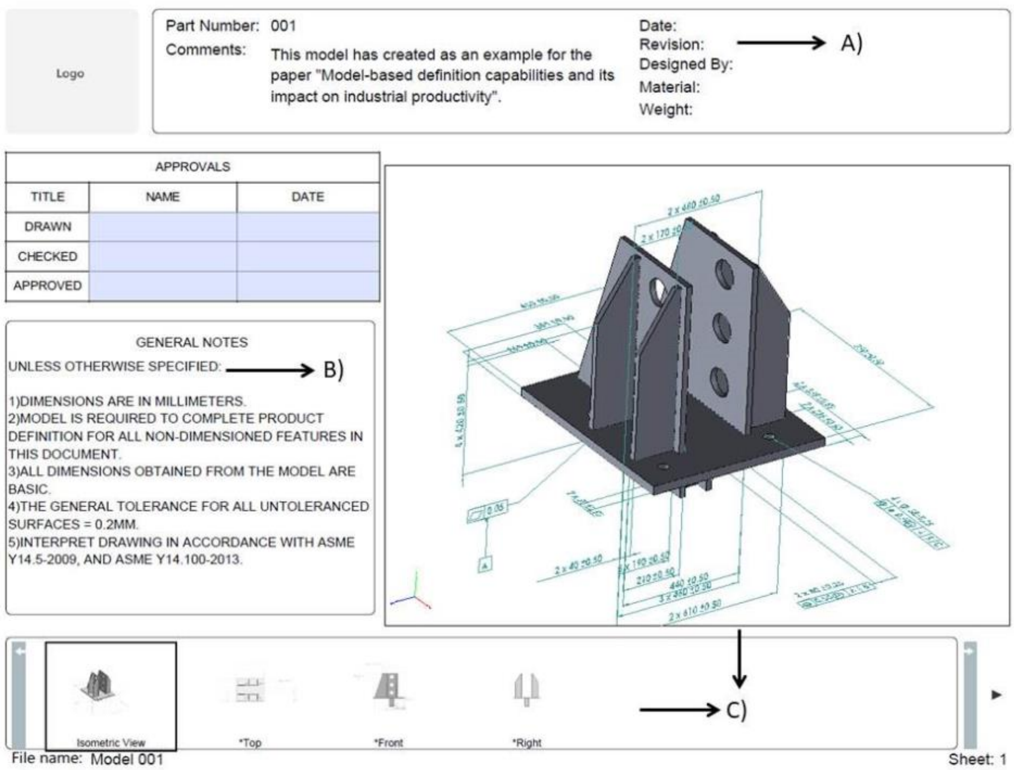

Figure 18. Example of MBD data in 3D PDF format (Varitis et al. 2020, p. 5).

For avoiding misconceptions, compliance of international standards is needed when creating engineering drawings. When using MBD-technology in case of complex assemblies, there can be challenging task to be able to define dimensions and annotations according to strict rules even for experienced user. The same problem occurs also when the dimensioning is verified. Another concern relates to storage of the document. Usually, drawings or microfilmed documents are used for retaining the definition of the product in a safe way, which allows for example reuse. Also, liability issues require a proper storage of the documents. Those aspects set requirements that needs to be considered if MBD is replacing traditional drawings. (Quintana et al. 2010, pp. 501-502; Varitis, et al. 2020, pp. 4-5.)

In general, the model-based definition is still in adoption phase, and it takes time for companies to adapt the technology. It requires sort of a cultural change, by determining new practices and guidelines. However, it has potential for gaining success among manufacturers as a part of the transformation for digital design and manufacturing. (Quintana et al. 2010, p. 502; Nguyen 2021.)

5 PARAMETRIC 3D-MODEL FOR LIME KILN SHELL SECTION

In this chapter, the development of parametric 3D-model for lime kiln shell section is presented. The development work was done by using Autodesk Inventor software. The model is designed for the needs of Andritz Oy, and it can be used as an auxiliary tool for lime kiln shell section change repair work documentation.

5.1 Demands for the model

The main goal of the 3D-model is to design and create manufacturing drawings for new shell section of the lime kiln based on the certain user input. The model should be able to create differently structured shell sections, with different length, size, thicknesses, and other accessories. The model needs to have ability to:

- modify shell inner diameter, kiln incline and kiln length,
- control plate thicknesses of shell plates,
- locate the shell section on correct position along kiln length,
- change included shell components, and their geometries,
- modify activity of riding ring and its type and geometry,
- control activity of filler bar structure and be able to modify its design effectively,
- control quantity and type of connection devices and locate them into correct seams,
- include the whole kiln shell geometry (as a reference), including other riding rings and girth ring.

Andritz has kiln series of standard kilns which is the base of dimensioning. However, in repair works the old kilns are not necessarily standard sizes and some customizations have been made or the standard sizing has changed over the years. In addition, the kilns that the service job is executed for might not necessarily be Andritz kilns. Also, for the section change repair, the new shell and components are basically designed again based on the old kiln conditions for example. For those reasons, the different dimensions and component combinations needs to be heavily customizable for ensuring proper usage of the model.

5.2 Parameters and user interface

Based on the demands, different parameters are determined for the model that user can control. The parameters are controlled with Microsoft Excel file, where the user can modify the template model for specific projects. For determining the correct position for the shell section and reference kiln dimensions, span lengths of the kiln need to be controlled by parameters. From figure 19 can be seen span lengths and support sections as general level. The span lengths are presented in capital letters A-F.

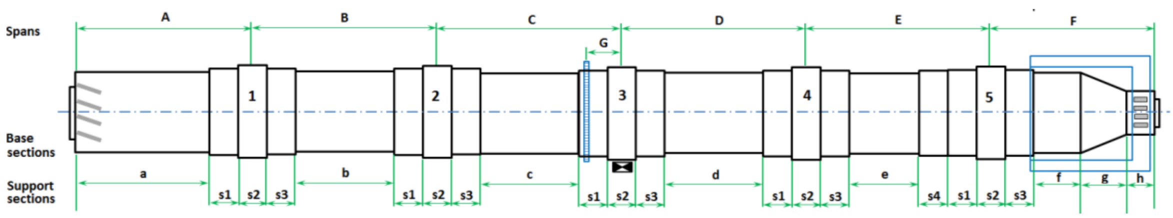

Figure 19. Span lengths of the kiln.

As can be seen from the figure 19, the different shell plates at support section are named as s1, s2, s3, s4, s5, where s2 is heavy shell under riding ring and s1, s3, s4 and s5 are flanker plates. The same naming principle is used for the shell section that can be seen in figure 20, where schematic picture of template shell section is shown. Also, thin shells are named with the same pattern, where s6 is thin shell at feed end side, and s7 at fire end side. From the figure can be seen that the seams are named by numbers 1-8. That is because the seams also must be identified for determining site welded seams and workshop welded seams.

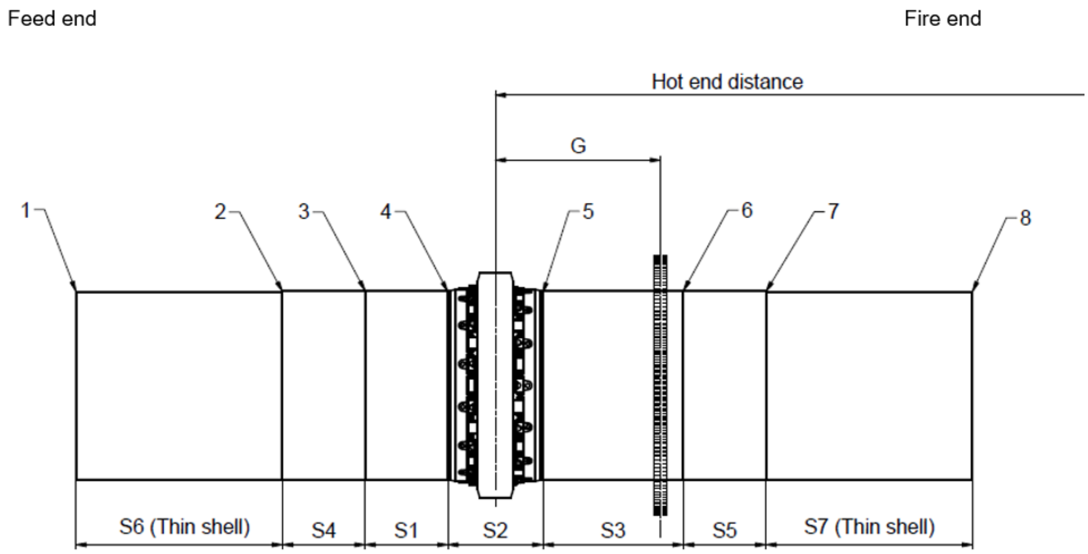

Figure 20. Shell section members.

The activity of shell plates needs to be parametrized because the needed combination differs depending the case. Also, riding rings, filler bar structure and wearing pieces must have activity parameter, because there could be projects where only thin shell is needed. In addition of activity, components need to have other parameters. Shell plates needs thicknesses, widths, and inner diameter to be parametrized. In addition, thin shell plates also need distance parameter from support location, if the replacement is wanted at the middle of span for example. Riding rings need parameters for inner and outer diameter, and guiding riding ring must have parameter for contact angle and contact height against the thrust bearing. Filler bar structure has many changing properties, and the structure basically must be designed for each case individually. That is why the dimensioning of filler bar structure is not automatized. Only general properties, width length thickness and quantity are determined at the Excel environment. Detailed designing is more sensible to done manually in the model.

The user interface is implemented to Excel file where the control of the template model is occurring. The Excel file consists of user input sheet and database sheet. The database sheet has all the Andritz standard kilns and their dimensions of shell thicknesses, shell lengths, span lengths and riding ring dimensions for both gas fired and oil fired kilns. From the database, default values of the selected kiln are collected for the input data sheet. The modification of the template model occurs in input data sheet. User selects the wanted configuration by using dropdown menus and edit value fields. The input data sheet of user interface can be seen in appendix I.

5.3 Structure of the model

The model is constructed based on top-down skeleton method, where the different components are controlled and linked to certain master file. The structural diagram of the model is shown in figure 21. The model consists of master skeleton file, one sub-skeleton, 17-part files, three sub-assemblies and one main assembly. In addition, there are three standard assemblies that are included to the structure. From the structural diagram, relations between components can be seen. Excluding the standard parts/assemblies all the components are related to master skeleton, *shell section skeleton*, which controls the model. The benefit for these relations between components is that modifications and changes occur in every level when the master skeleton changes. In addition, there is no need for using constraints between components at assembly level because the parts are generated initially at the correct location. That is beneficial because the constraints tend to be broken when modifications are made which causes errors.

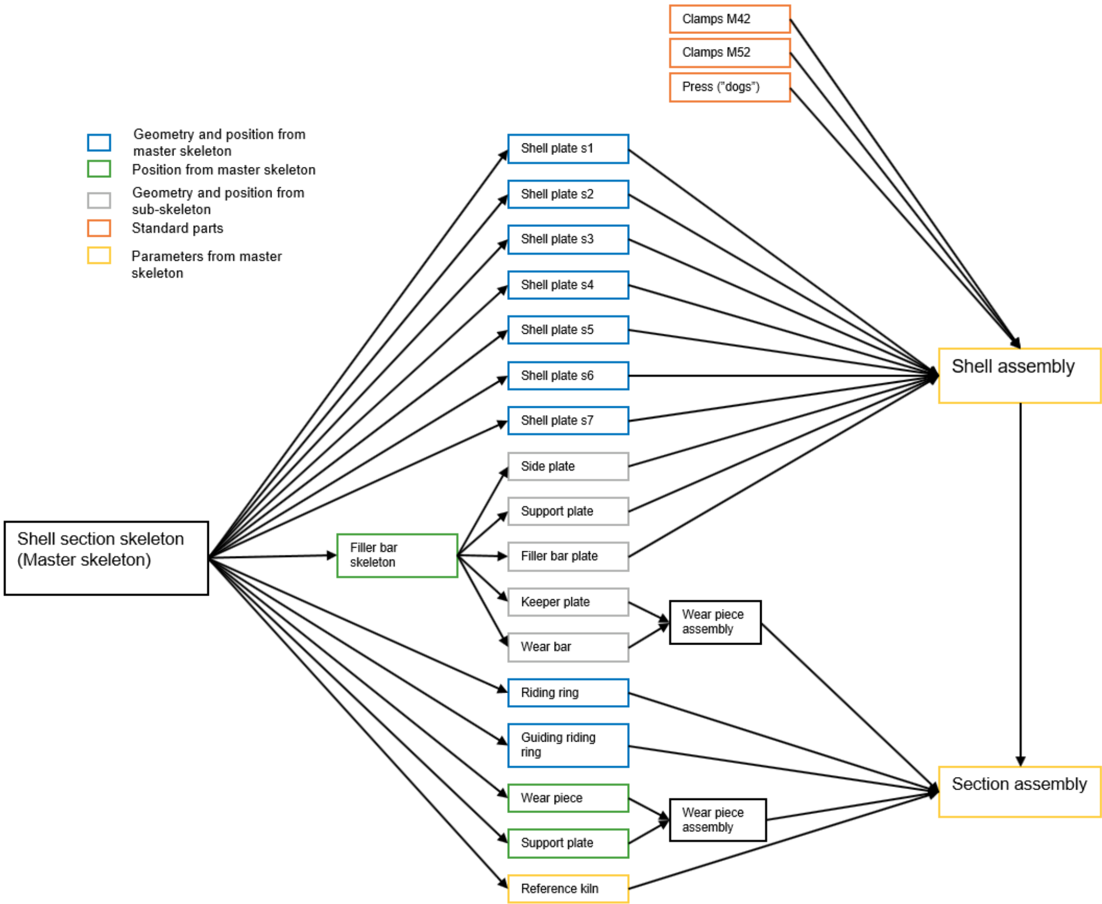

Figure 21. Structural diagram of the model.

There are five different relationships used in model structure which are presented by color codes in structure diagram. Blue color presents relation where both geometry and position of the part is controlled by master skeleton. That means that the blank geometry of the part is created from skeleton model for the correct location in the coordinate system. The specific features of the parts are made in the part file level. Green color presents relation where the position of the part in the coordinate system is determined based on skeleton model. That means that the geometry of the part is created at the part file level, but position is derived from skeleton file by planes or parameters that are used for creating geometry at correct position. Yellow color means that only parameters are linked from skeleton file. That is used for assemblies that uses the parameters for controlling patterns and iLogic functions. Orange color means that particular components are standard components, and they are not linked to skeleton in any way. For that reason, they need constraints for determining relations to other components.

The parameter file and user interface that was presented in chapter 5.2 is linked to the master skeleton. That way the data from excel flows through the whole model. The skeleton model is shown in figure 22. As can be seen from the figure, blank geometries of shell plates and riding ring are created at skeleton model. The shell section is positioned based on hot end of the kiln, which is determined to be at origin of the coordinate system. Because the standard parts are not created by deriving from skeleton, there is determined features (geometry planes and surfaces) for the skeleton, that can be used for constraining those parts. That way, the standard parts can be constrained to skeleton model, so the relation doesn’t break when the assembly configuration changes.

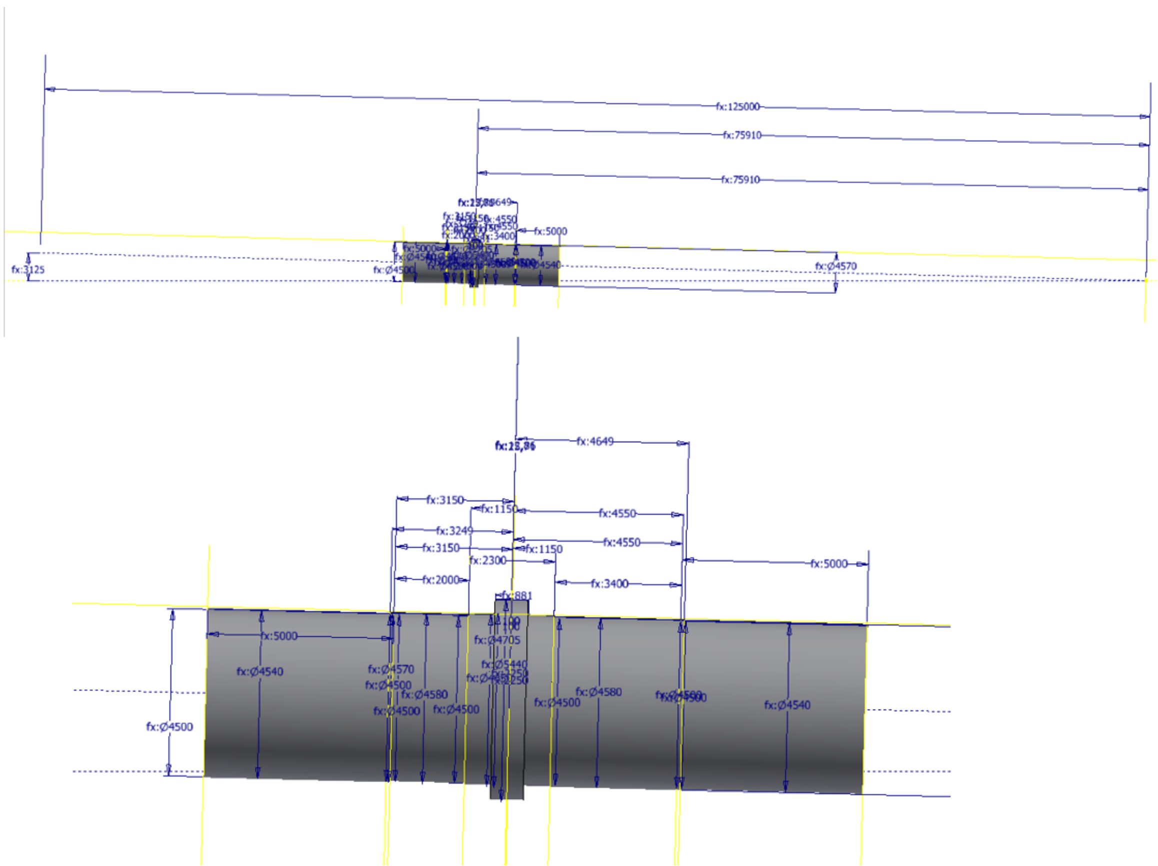

Figure 22. Master skeleton of shell section model.

As was presented earlier, the model also contains one sub-skeleton. The sub-skeleton controls dimensions of filler bar structure. Because the filler bars have many possible configurations and dimensions, the structure was decided not to be automatized. That way main parameters, quantity, thickness, length and width, are determined at the user interface but the detailed dimensioning is occurring at model phase by modifying the sub-skeleton. The sub-skeleton allows to have visual representation along with the design, so for example distances between components can be detected efficiently. The filler bar skeleton (figure 23) creates the geometry of the filler bar structure components and positions them in correct location at the coordinate system. However, the same component can only have one part file and the components are used for multiple times at assemblies, so the origin-based positioning can be done only for one of those parts. Other members are positioned with pattern features by utilizing auxiliary geometries, for example axes.

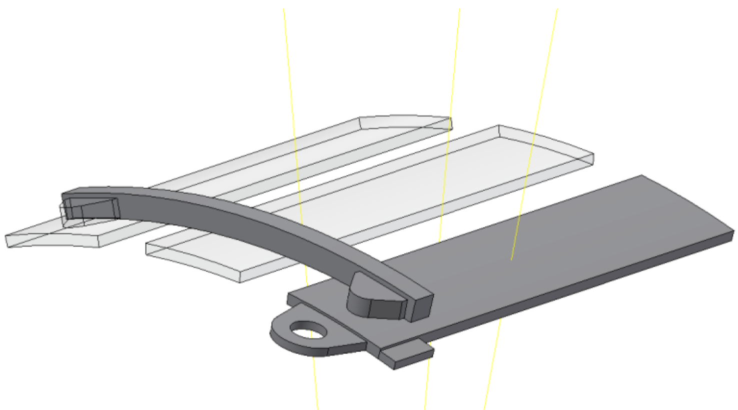

Figure 23. Filler bar skeleton.

Created parts are united into assemblies according to structural diagram that was shown in figure 21. As most of the parts are created based on common origin, they do not need constraints with each other. Only standard parts are positioned by constraints. The template model has need for adapting different configurations that the user has defined. For that reason, those assemblies include all the parts that the structure may need even though they are never used at the same time. The wanted configuration is then formed with Inventor's level of detail selection which allows to suppress components and assemblies that are not needed. The control of the level of detail is done by utilizing iLogic-coding, that creates the correct level of detail automatically based on user defined parameters.

iLogic is Inventor's own programming environment that can be used for controlling 3D-model files. It is designed to be user friendly in a way that it can be used without having strong programming skills. It has pre-defined functions that can be controlled for example, by basic If-Then-Else-statements. (Autodesk 2019.)

In this model, the iLogic is used in two assemblies, *shell assembly* and *section assembly*, for determining active components and features of the assemblies. For the table 1 is collected features, that iLogic is used to control in assemblies.

Table 1. iLogic driven features at model.

Shell assembly
Activity of shell plates
Machining shape of heavy shell plate
Connection device type and installation seams (location of connection devices)
Activity of filler bar structure
Section assembly
Activity of riding ring
Type of riding ring
Type of wear piece

The iLogic-rules of the model are using parameters that were defined at excel file. The most used function is *component.IsActive("part name")* which basically suppress or unsuppress determined component. One example of determined iLogic-rule is shown in figure 23 which controls activity and type of riding ring. It consists of conditional statements on two level, where the code first determines if the riding ring is included. If the parameter for that is "0", the rule suppresses both riding rings from the model. If it is "1", the code checks parameter of riding ring type. Depending on that, the rule suppresses the unwanted ring from the model.

```
If Riding_Ring_Is_Active = 1.000 ul Then

    If Riding_Ring_Type = 1.000 ul  Then
        Component.IsActive("LK_Shell_Section_Guiding_Riding_Ring_(Do_Not_Rename)") = True
        Component.IsActive("LK_Shell_Section_Riding_Ring_(Do_Not_Rename)") = False

    ElseIf Riding_Ring_Type = 2.000 ul  Then
        Component.IsActive("LK_Shell_Section_Guiding_Riding_Ring_(Do_Not_Rename)") = False
        Component.IsActive("LK_Shell_Section_Riding_Ring_(Do_Not_Rename)") = True

    End If

ElseIf Riding_Ring_Is_Active = 0.000 ul   Then
    Component.IsActive("LK_Shell_Section_Guiding_Riding_Ring_(Do_Not_Rename)") = False
    Component.IsActive("LK_Shell_Section_Riding_Ring_(Do_Not_Rename)") = False

End If
```

Figure 24. iLogic-rule for riding ring activity and type.

The top-level assembly of the model is the *section assembly*, which is shown in figure 25. It includes the components which user was defined for the excel file. In addition, the assembly includes rest of the kiln shell as a reference without detailed geometries. That provides better visual observation of the configuration. It also shows for example, where the section locates at the kiln and which size of kiln is dealt with in general.

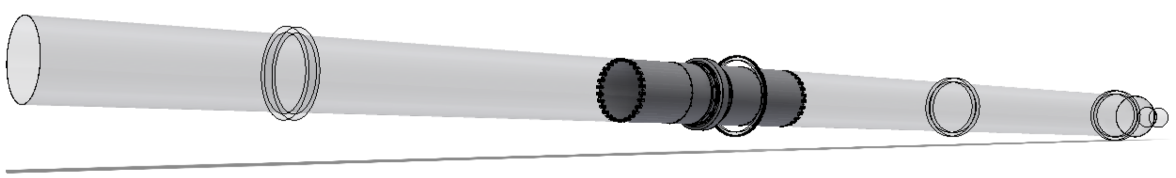

Figure 25. Top level assembly.

Drawings are made for all the assemblies and riding rings. For the assemblies that have heavily modifying geometry and configuration, automating the dimensioning process for drawings is complex because the references where initial dimensioning is done, could disappear. For that reason, the dimensioning of the drawing is not automated, and user needs to do it manually. However, the drawings are prepared in a way that needed projections are created automatically. That speeds up the drawing processes compared to blank drawing sheet.

The functionality and quality of the template model is tested with different variations and cases. The model functionality is evaluated based on the tests by user experience of the model. In other words, the model is evaluated is it capable for creating the required documents that it was meant to. The effectiveness is analyzed by measuring time phases that the usage of model consumes. That way the challenging properties can be identified and improved for future development.

6 EFFECT OF SHELL AXIS MISALIGNMENT ON SUPPORT LOADS

In this chapter, the phenomena where axis misalignment is occurred at the shell is studied. Focus of the study is on the effect to support forces of the kiln and bending stresses at the shell when the axis misalignment is present. The phenomenon is observed by conducting structural analyzes of the misalignment state by Ansys Workbench software.

6.1 Description of analysis

As presented in chapter 3.4, the kiln shell might occasionally have misalignment where the centerline of the shell is not straight. That can happen for example, because of sinking of foundations or wearing of the riding ring, that changes the centerline position at support. In this work, situation is studied where one of the supports are either sunken or elevated from the lining, and how it affects to the support forces and bending stresses at different supports. The change of support forces can be critical because increase of the loadings can lead to bearing damage for example. Also, if the bending stresses are at increased level for a long time, damage for the shell may occur. As a limit for the allowable increase of support forces is determined to be 10%, which can be considered to cause problems with support roller bearings if it is exceeded. The situation is studied, by modelling the misalignment for the shell and calculating the caused support loads. The misalignment is modelled for different piers for different direction for getting the impact of the location and direction of the misalignment into account. The analyses are made for different sized kilns, because the phenomenon occurs differently depending on the number of supports. Used kiln sizes are 5,5 m x 165 m, which has five supports, and 3,4 m x 90 m, which has three supports.

6.2 Ansys beam-model

The analysis is made by Ansys Workbench software, where the different situations are modelled. Modelling starts by creating geometry of the kiln shell. Because beam element type is used, geometry is modelled as lines where the cross-sections are determined. Different cross-sections have their own line geometry, so lengths of the lines are determined specifically. Geometries of Ansys-models for kiln 5,5 m x 165 m and 3,4 m x 90 m are shown in figure 26. From the figure can be seen the cross-section changes at the support locations.

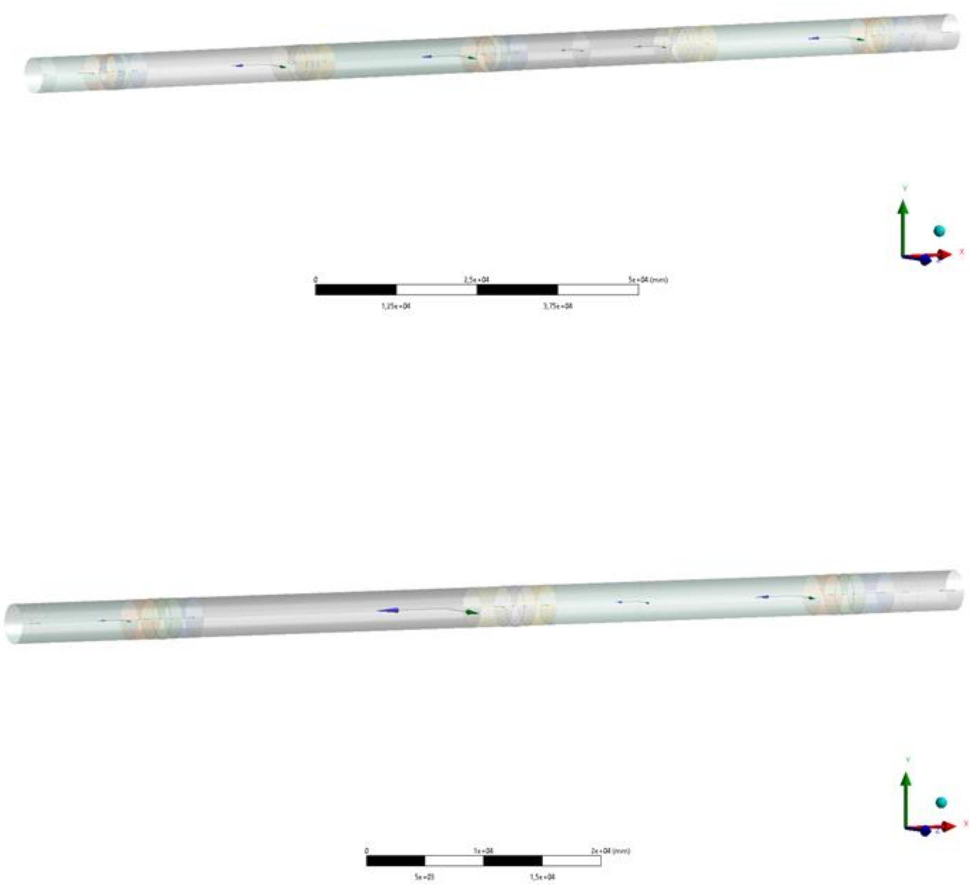

Figure 26. Geometries of the models: 5,5 m x 165 m (top), 3,4 m x 90 m (bottom).

Meshing is done by beam elements, in a way that the heavy shell and flanker plates have smaller element sizes. That is because the results are wanted to be more accurate at the support locations. The beam elements are considered to have enough accuracy for this analysis, because the studied results are at relatively global level, which means the deformation of the cross-section is not under observation for example. That might reduce the accuracy of the absolute values of the results, but that is not considered to be a problem, because the relative change of the loadings is under observation.

The loadings for the model are determined accurately for simulating the real situation. Because of the large mass of the structure, own weight of the steel shell is taken into account.

It is considered by inserting standard gravity force for the analysis. The refractory lining inside the shell, has significant effect of the total loads of the kiln. That is why it needs to be inserted accurately. The refractory is divided to different zones along the length of the shell. Different zones have different refractory properties, so the refractory loadings differ along the length of the shell. There are six different refractory zones that have different lengths depending on the kiln size. For both models, the shell geometry is divided based on the different refractory zones. That way the specific refractory load can be determined as a line force based on the zone location. The weight of the cooler needs to be inserted for the model because of its significance. Also, the analysis is simulating operating conditions which means that the weight of the lime mud that is going through the kiln is noticed. The lime load is inserted along the length of the kiln and added to the weight of the cooler. In addition, point loads are inserted to both ends of the shell, that are representing weights of feed end and discharge end necks. For both models there is total of ten loads determined.

The model is constrained from the support locations of the kiln. The constraint type that is used is simply supported, which restrains the displacements but allows rotations. However, for the support that is determined to be sunken or elevated, the simply supported constraint is replaced with forced displacement. That way the effect of misalignment of the shell can be simulated. The different displacement scenarios for the kiln 5,5 m x 165 m are presented in figure 27. The displacement is set for support 2 and support 3 for sunken and elevated directions as seen from figure.

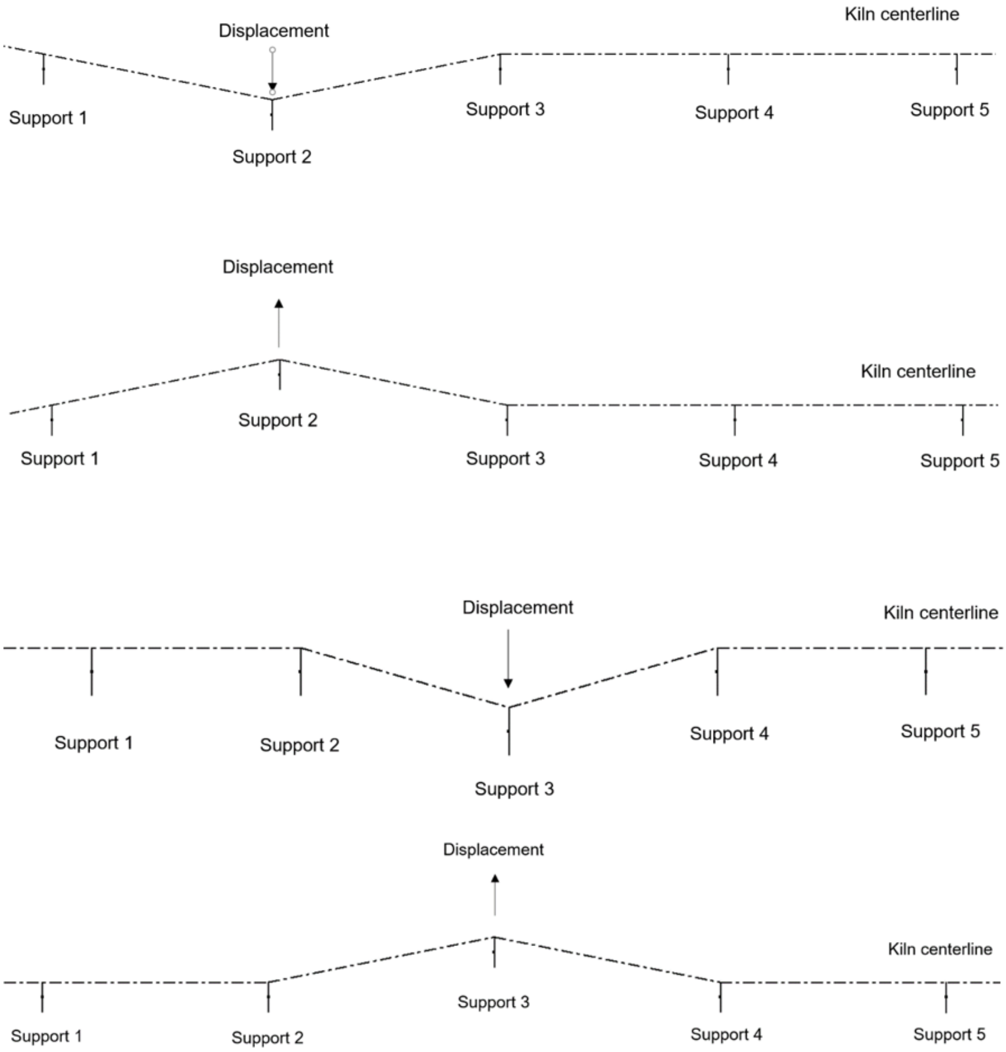

Figure 27. Displacement scenarios for kiln 5,5 m x 165 m.

Different displacement scenarios for three-support kiln 3,4 m x 90 m can be seen in figure 28. Similarly, as with the larger kiln the displacement is set for sunken and elevated direction. However, the displacement is set for support 1 and support 2 for the three-support kiln as can be seen in figure. For each case for both kilns, 1 mm steps of increase were made until the 10% of increase on support forces is reached in any of the supports.

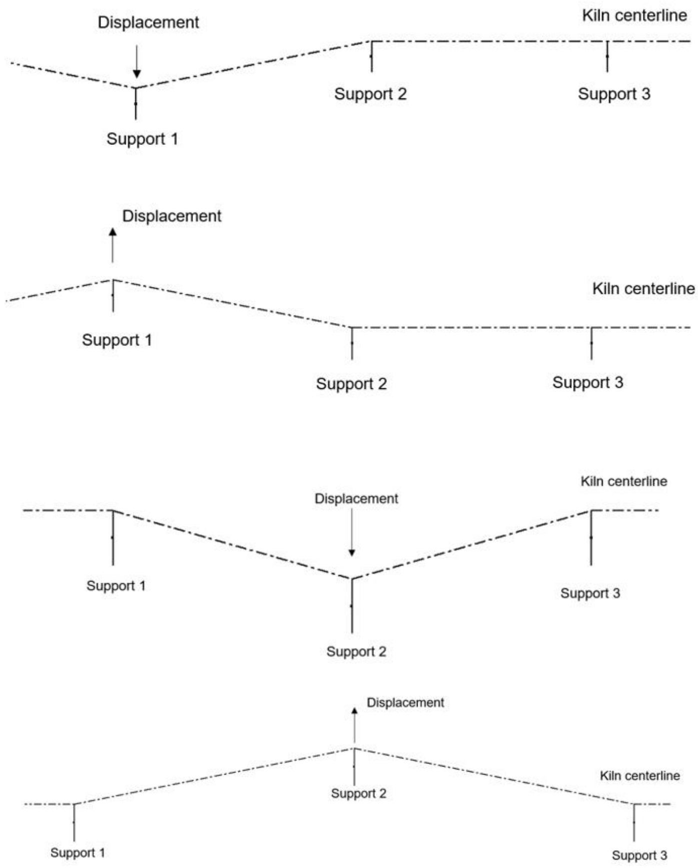

Figure 28. Displacement scenarios for kiln 3,4 m x 90 m.

Linear static structural analyzes were made for the two models. For each analysis, support forces and bending stresses were collected from each of the support. The results were then processed in a way that the weights of the riding rings were added to the support forces, and the changes of the support loads were compared to initial state. Initial state of bending moment distribution for kiln 5,5 m x 165 m is shown in figure 29. The fire end of the kiln is at the 0 mm and the feed end at the -165000 mm.

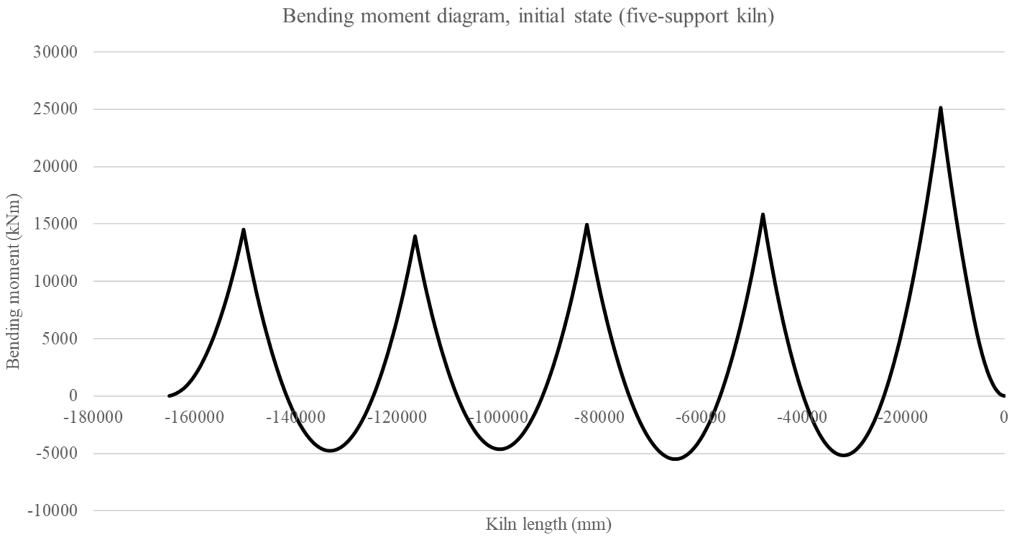

Figure 29. Bending moment diagram for kiln 5,5 m x 165 m without misalignment.

Bending moment diagram for kiln 3,4 m x 90 m at initial state without axis misalignment is shown in figure 30. Similarly, as with the moment diagram of five-support kiln, the fire end is at the 0 mm and feed end at the -90000 mm.

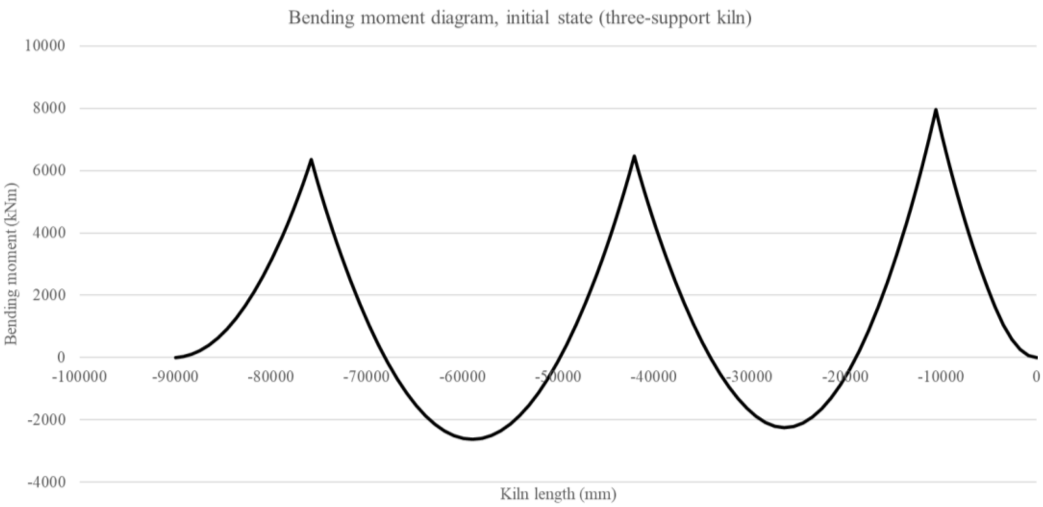

Figure 30. Bending moment diagram for kiln 3,4 m x 90 m without misalignment.

7 RESULTS

In this chapter, results of the experimental part of the work are presented. The work included creation of template 3D-model for lime kiln shell section which quality and functionality are presented. Another part of the work was to study the effect of kiln axis misalignment on support loads which was concluded by FE-analysis. Results of the conducted analyzes are presented also.

7.1 Quality of 3D-template model

The shell section 3D-model was tested with different scenarios and it turned out that the model can be used for designing lime kiln shell section for section change project. With usage of the model, correct configuration of the structure and its drawings were able to be produced. For the performance perspective, the 3D-model for wanted configuration was created automatically based on input values, and it is able to produce the wanted version of the assembly. Occasionally the model and some features doesn’t update correctly at first, and it seems visually incorrect. However, those bugs get fixed when the feature, for example pattern, was updated again.

The 3D-model doesn’t create drawings automatically, which requires the most manual work. With single parts, and small assemblies the drawings are almost correct automatically, and only small modifications are needed. For the larger assemblies, the model creates automatically correct projections of the model, but dimensioning needs done be done manually. Also, depending on the configuration, the drawing sheet has extra projections that needs to be removed. From outside of the drawing sheet, some sample images were inserted that helps the user for dimensioning correctly. In addition, for supporting the usage of the template model, design instructions were created, which has information of the work procedure and structure of the model. It also guides the user for creating correct drawings.

During test use of the model different phases were clocked for analyzing the effectiveness of it. The work times are presented in table 2, where the model is divided into three main sections and seven sub-sections. Creation of 3D-model consists of following subfaces. Preparation of template model, that includes copying and renaming the model into correct file. Input of initial values, that includes setting up the user interface with correct dimensions and selections. Review and modification of the model, that includes the updating the model with modified input parameters, checking that the model seems correct and possible modifications that are made if needed. Also, the detailed dimensioning of the filler bar structure is included in that section. Creation of drawings includes the needed drawings that are made for shell assembly, riding ring, wear pieces and section assembly. Setting of material properties includes the determination of material codes for each part and checking that the part lists is correct. Each section time of work of is shown in percentages.

Table 2. Time of work phases of 3D-model.

Phase		**Time of work phase**	
Creation of 3D-model	Preparation of template model	4 %	22 %
	Input of initial values	5 %	
	Review and modification of the model	13 %	
Creation of drawings	Shell assembly drawing	30 %	61 %
	Riding ring drawing	4 %	
	Wear piece drawing	3 %	
	Section assembly drawing	24 %	
Setting of material properties			17 %

From the table can be seen that preparation of the template model takes 4% of the time, feeding of input values takes 5%, review and modification of the model takes 13% of the time which makes the total time portion of model creation phase of 22 %. For the drawings, the total time of modification and dimensioning was 61 %, which was divided in a way that shell assembly drawing takes 30 %, section assembly 24 % riding ring 4% and wear pieces 3%. In addition, material property determination and checking of part list have 17 % of the time.

7.2 The effect of axis misalignment

FE-analyzes were made as was introduced in chapter 6, where the effect of kiln axis misalignment on support forces is analyzed. The effect was studied by modelling the misalignment by forced displacements for different values at different locations. The calculations were made for kiln 5,5 m x 165 m and for kiln 3,4 m x 90 m. For both kilns the misalignment was calculated at two supports in a way that the displacement was placed for both directions along vertical axis. Collected results from the analyzes were the changes on support forces and bending stresses for shell at support locations. All the results can be found on appendix II, and the most important ones are presented next.

7.2.1 The effect on support forces for kilns 5,5 m x 165 m and 3,4 m x 90 m

The results are presented in a way that for both kilns, each displacement results are collected to own table. Tables presents the change of support forces when 1 mm displacement is occurred, and when the increase of support force reaches 10% at any support. The values are compared to initial state, where the supports are on a straight line. Colors represents the direction of the change of values in a way that red color means increase of support force and green color decrease of support force. From the table 3 can be seen the changes of support forces for kiln 5,5 m x 165 m when the displacement occurs at support 2 for a downward direction. The most increase occurs at support 3, where the increase on support force is 1,5% for 1 mm displacement. That way the 10% increase occurs at 7 mm of sinking at support 2.

Table 3. Change of support forces for kiln 5,5 m x 165 m. Displacement at support 2, negative vertical direction.

Displacement (Support2)	**Change of support forces [%]**				
(mm)	**Support 1**	**Support 2**	**Support 3**	**Support 4**	**Support 5**
0	0,0%	0,0%	0,0%	0,0%	0,0%
-1	0,6%	-1,6%	1,5%	-0,5%	0,1%
-6	3,8%	-9,8%	8,8%	-3,2%	0,4%
-7	4,5%	-11,4%	10,3%	-3,8%	0,5%

For the table 4 has been collected the changes of support forces for kiln 5,5 m x 165 m when the displacement occurs at support 2 for upward direction. The most increase occurs at support 2, where the increase of support force is 1,6% for 1 mm displacement. The 10% increase is reached at 7 mm of displacement.

Table 4. Change of support forces for kiln 5,5 m x 165 m. Displacement at support 2, positive vertical direction.

Displacement (Support2)	**Change of support forces [%]**				
(mm)	**Support 1**	**Support 2**	**Support 3**	**Support 4**	**Support 5**
0	0,0%	0,0%	0,0%	0,0%	0,0%
1	-0,6%	1,6%	-1,5%	0,5%	-0,1%
6	-3,8%	9,8%	-8,8%	3,2%	-0,4%
7	-4,5%	11,4%	-10,3%	3,8%	-0,5%

The changes on support forces for kiln 5,5 m x 165 m when the displacement is affecting at support 3 for downward direction are presented in table 5. The most increase occurs at support 2, where it is 1,6% for 1 mm displacement. That way the 10% increase is reached when the displacement is 7 mm.

Table 5. Change of support forces for kiln 5,5 m x 165 m. Displacement at support 3, negative vertical direction.

Displacement (Support3)	**Change of support forces [%]**				
(mm)	**Support 1**	**Support 2**	**Support 3**	**Support 4**	**Support 5**
0	0,0%	0,0%	0,0%	0,0%	0,0%
-1	-0,5%	1,6%	-2,1%	1,3%	-0,3%
-6	-2,7%	9,3%	-12,6%	7,7%	-1,7%
-7	-3,1%	10,9%	-14,7%	8,9%	-1,9%

The changes of support forces for the kiln 5,5 m x 165 m, when displacement is at support 3 for upward direction are shown in table 6. The most increase occurs at support 3, where it is 2,1% for a 1 mm displacement. The 10% increase of support forces is then reached at 5 mm elevation at support 3.

Table 6. Change of support forces for kiln 5,5 m x 165 m. Displacement at support 3, positive vertical direction.

Displacement (Support3)	**Change of support forces [%]**				
(mm)	**Support 1**	**Support 2**	**Support 3**	**Support 4**	**Support 5**
0	0,0%	0,0%	0,0%	0,0%	0,0%
1	0,5%	-1,6%	2,1%	-1,3%	0,3%
4	1,8%	-6,2%	8,4%	-5,1%	1,1%
5	2,2%	-7,8%	10,5%	-6,4%	1,4%

For the table 7 is collected changes of the support forces for kiln 3,4 m x 90 m when displacement occurs at support 1 for downward direction. The maximum increase occurs at support 2, where it is 0,3% for 1 mm displacement. 10% increase occurs when the displacement at support 1 is 40 mm.

Table 7. Change of support forces for kiln 3,4 m x 90 m. Displacement at support 1, negative vertical direction.

Displacement (Support1)	**Change of support forces [%]**		
(mm)	**Support 1**	**Support 2**	**Support 3**
0	0,0%	0,0%	0,0%
-1	-0,1%	0,3%	-0,1%
-2	-0,3%	0,5%	-0,2%
-40	-5,3%	10,0%	-4,4%

The changes of support forces for kiln 3,4 m x 90 m when the displacement occurs at support 1 for upward direction are presented in table 8. The biggest increase occurs at support 1 where it is 0,1% for 1 mm displacement. That way the 10% increase occurs at 76 mm elevation of the support 1.

Table 8. Change of support forces for kiln 3,4 m x 90 m. Displacement at support 1, positive vertical direction.

Displacement (Support1)	**Change of support forces [%]**		
(mm)	**Support 1**	**Support 2**	**Support 3**
0	0,0%	0,0%	0,0%
1	0,1%	-0,3%	0,1%
2	0,3%	-0,5%	0,2%
76	10,1%	-19,0%	8,3%

The effect of the displacement at support 2 for downward direction for kiln 3,4 m x 90 m support forces is shown in table 9. The highest increase occurs on support 1, where 1 mm displacement causes 0,3% growth on support forces. That way the 10% increase is reached when the displacement is 37 mm.

Table 9. Change of support forces for kiln 3,4 m x 90 m. Displacement at support 2, negative vertical direction

Displacement (Support2)	**Change of support forces [%]**		
(mm)	**Support 1**	**Support 2**	**Support 3**
0	0,0%	0,0%	0,0%
-1	0,3%	-0,5%	0,2%
-2	0,6%	-1,0%	0,5%
-37	10,2%	-19,2%	8,4%

For the table 10 has been collected the changes of support forces for kiln 3,4 m x 90 m when the displacement occurs at support 2 for elevated direction. From the table can be seen that the largest increase occurs at support 2 where 1 mm displacement causes 0,5% increase of support force. That way the 10% growth is reached at 20 mm displacement.

Table 10. Change of support forces for kiln 3,4 m x 90 m. Displacement at support 2, positive vertical direction.

Displacement (Support2)	**Change of support forces [%]**		
(mm)	**Support 1**	**Support 2**	**Support 3**
0	0,0%	0,0%	0,0%
1	-0,3%	0,5%	-0,2%
2	-0,6%	1,0%	-0,5%
20	-5,5%	10,4%	-4,5%

7.2.2 The effect on bending stresses at support locations for kilns 5,5 m x 165 m and 3,4 m x 90 m

The changes of bending stresses are collected in a similar way as the support forces. The changes of bending stress values are presented at support locations, with the same displacements that were used previously. That way both, support forces and bending stresses can be collected when the same displacement is occurring. From the table 11 can be seen the changes of bending stresses for the kiln 5,5 m x 165 m when the displacement occurs at support 2 for downward direction. The most increase occurs at support 3 where it is 5,1% for 1 mm. At 7 mm displacement, when the support force increased 10%, the bending stress has increased 35,8%.

Table 11. Change of bending stresses at support locations for kiln 5,5 m x 165 m. Displacement at support 2, negative vertical direction.

Displacement (Support2)	**Change of bending stress [%]**				
(mm)	**Support 1**	**Support 2**	**Support 3**	**Support 4**	**Support 5**
0	0,0%	0,0%	0,0%	0,0%	0,0%
-1	0,0%	-7,8%	5,1%	-1,2%	0,0%
-6	0,0%	-46,5%	30,7%	-7,3%	0,0%
-7	0,0%	-54,2%	35,8%	-8,5%	0,0%

The changes of bending stresses for the kiln 5,5 m x 165 m when the displacement occurs at support 2 for upward direction is shown in table 12. The biggest increase is at support 2 where it is 7,7% for 1 mm displacement. At 7mm displacement, where the support force increased 10%, the increase of bending stress is 54,2%.

Table 12. Change of bending stresses at support locations for kiln 5,5 m x 165 m. Displacement at support 2, positive vertical direction.

Displacement (Support2)	**Change of bending stress [%]**				
(mm)	**Support 1**	**Support 2**	**Support 3**	**Support 4**	**Support 5**
0	0,0%	0,0%	0,0%	0,0%	0,0%
1	0,0%	7,7%	-5,1%	1,2%	0,0%
6	0,0%	46,5%	-30,7%	7,3%	0,0%
7	0,0%	54,2%	-35,8%	8,5%	0,0%

Bending moment and bending stress diagrams for kiln 5,5 m x 165 m when displacement is occurring at support 2 are shown in figure 31. The diagram shows bending moment and stress without axis misalignment, and with the displacements that increases support forces by 10%.

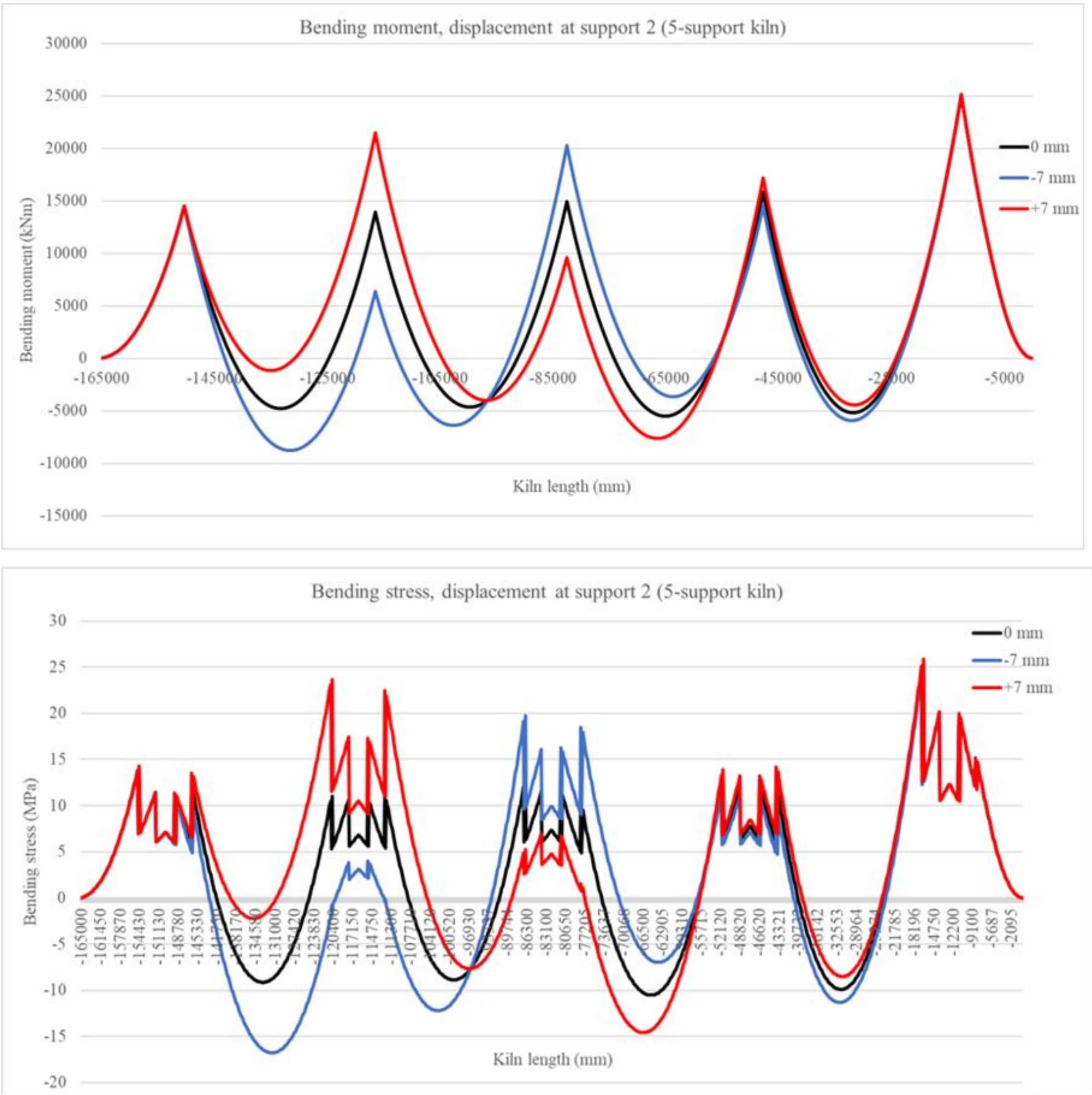

Figure 31. Bending moment and bending stress diagrams for kiln 5,5 m x 165 m, displacement at support 2.

For the table 13 has been collected the changes of bending stresses for the kiln 5,5 m x 165 m when the displacement is occurring at support 3 for downward direction. The largest increase occurs at support 2 where it is 5,5% for 1 mm displacement. At 7 mm displacement the increase of bending stress is 38,2%.

Table 13. Change of bending stresses at support locations for kiln 5,5 m x 165 m. Displacement at support 3, negative vertical direction.

Displacement (Support3)	**Change of bending stress [%]**				
(mm)	**Support 1**	**Support 2**	**Support 3**	**Support 4**	**Support 5**
0	0,0%	0,0%	0,0%	0,0%	0,0%
-1	0,0%	5,5%	-8,4%	4,6%	0,0%
-6	0,0%	32,8%	-50,4%	27,8%	0,0%
-7	0,0%	38,2%	-58,8%	32,4%	0,0%

From the table 14, changes of the bending stresses for kiln 5,5 m x 165 m can be seen when the displacement occurs at support 3 for upward direction. The largest increase occurs at support 3 where it is 8,4% for 1 mm displacement. At 5 mm displacement, the increase of bending stress is 42,0%.

Table 14. Change of bending stresses at support locations for kiln 5,5 m x 165 m. Displacement at support 3, positive vertical direction.

Displacement (Support3)	**Change of bending stress [%]**				
(mm)	**Support 1**	**Support 2**	**Support 3**	**Support 4**	**Support 5**
0	0,0%	0,0%	0,0%	0,0%	0,0%
1	0,0%	-5,5%	8,4%	-4,6%	0,0%
4	0,0%	-21,8%	33,6%	-18,5%	0,0%
5	0,0%	-27,3%	42,0%	-23,2%	0,0%

For kiln 5,5 m x 165 m, the bending moment and bending stress diagrams are shown in figure 32, when displacement is occurring at support 3. There can be seen the bending moment and stress without axis misalignment and with the displacements that causes 10% increase of support forces.

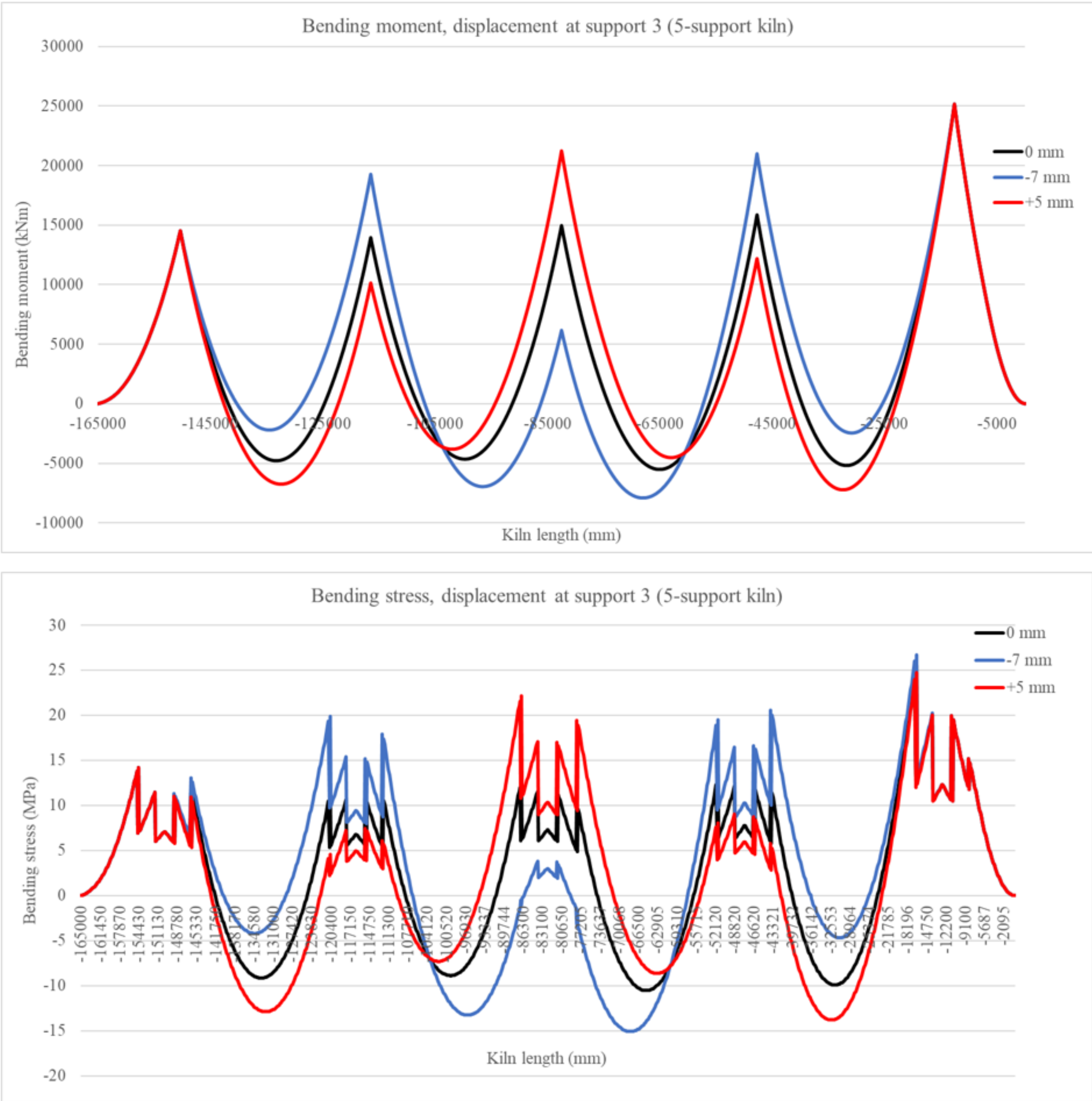

Figure 32. Bending moment and bending stress diagrams for kiln 5,5 m x 165 m, displacement at support 3.

Changes of the bending stresses of the kiln 3,4 m x 90 m when the displacement occurs at support 1 for downward direction is shown at table 15. The largest increase occurs at support 2 where it is 1,5% for 1 mm displacement. At 40 mm displacement the growth is 61,2% for the bending stress.

Table 15. Change of bending stresses at support locations for kiln 3,4 m x 90 m. Displacement at support 1, negative vertical direction.

Displacement (Support1)	**Change of bending stress [%]**		
(mm)	**Support 1**	**Support 2**	**Support 3**
0	0,0%	0,0%	0,0%
-1	0,0%	1,5%	0,0%
-2	0,0%	3,1%	0,0%
-40	0,0%	61,2%	0,0%

From the table 16 can be seen the changes of bending stresses for the kiln 3,4 m x 90 m when the displacement occurs at support 1 for upward direction. Bending stresses doesn't increase on any support but decrease at support 2. The decrease is 1,5% for 1 mm and 116,3% for 76 mm displacement.

Table 16. Change of bending stresses at support locations for kiln 3,4 m x 90 m. Displacement at support 1, positive vertical direction.

Displacement (Support1)	**Change of bending stress [%]**		
(mm)	**Support 1**	**Support 2**	**Support 3**
0	0,0%	0,0%	0,0%
1	0,0%	-1,5%	0,0%
2	0,0%	-3,1%	0,0%
76	0,0%	-116,3%	0,0%

For the figure 33 is collected bending moment and bending stress diagrams for kiln 3,4 m x 165 m when displacement is occurring at support 1. The diagram shows bending moment and stress without axis misalignment and with the displacements that causes 10% increase of support forces.

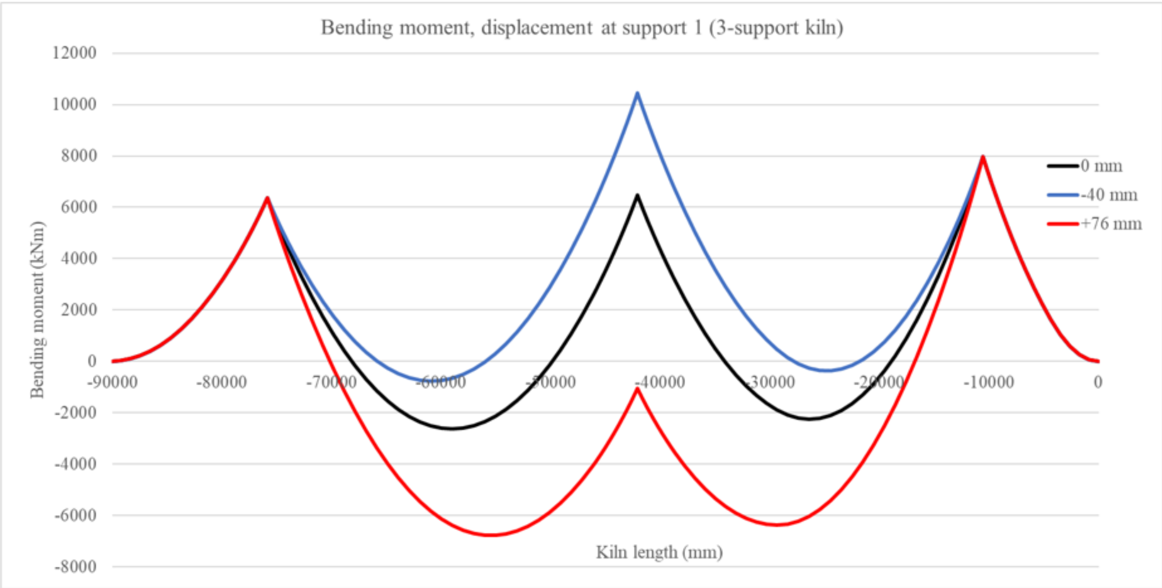

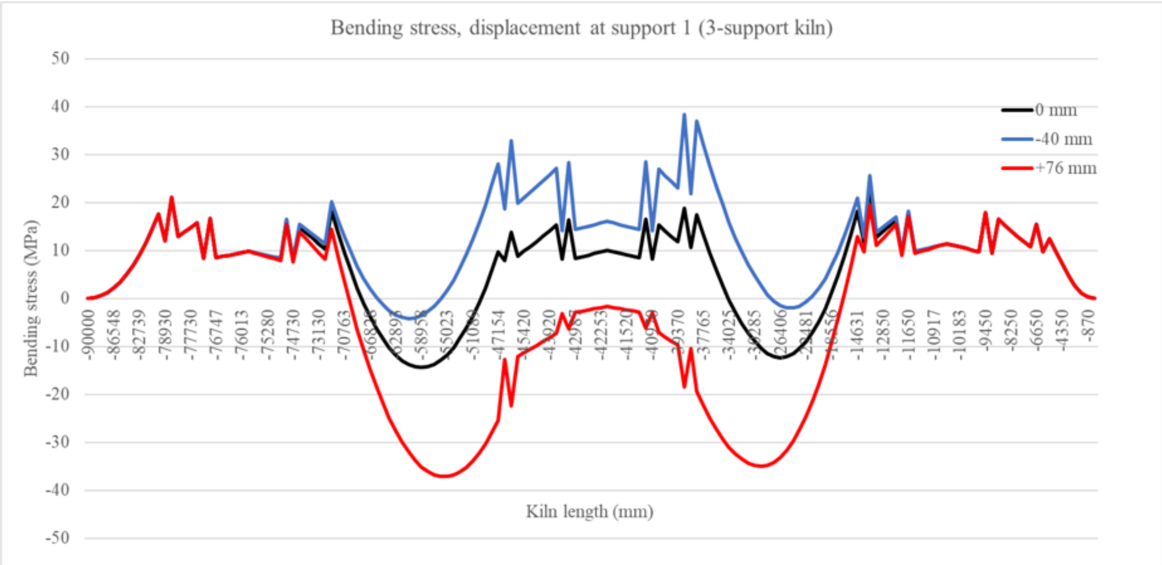

Figure 33. Bending moment and bending stress diagrams for kiln 3,4 m x 165 m, displacement at support 1.

The change of bending stresses for kiln 3,4 m x 90 m when the displacement occurs at support 2 for downward direction is shown in table 17. From the table can be seen that bending stresses doesn't increase at any support. Decrease is 3,2% at support 2 for 1 mm displacement and 117,2% for 37 mm displacement.

Table 17. Change of bending stresses at support locations for kiln 3,4 m x 90 m. Displacement at support 2, negative vertical direction.

Displacement (Support2)	**Change of bending stress [%]**		
(mm)	**Support 1**	**Support 2**	**Support 3**
0	0,0%	0,0%	0,0%
-1	0,0%	-3,2%	0,0%
-2	0,0%	-6,3%	0,0%
-37	0,0%	-117,2%	0,0%

For the table 18 is collected the changes of bending stresses for kiln 3,4 m x 90 m when the displacement occurs at support 2 for upward position. The increase of bending stresses occurs at support 2 where it is 3,2% for 1 mm displacement. At 20 mm displacement the increase is 63,4%.

Table 18. Change of bending stresses at support locations for kiln 3,4 m x 90 m. Displacement at support 2, positive vertical direction.

Displacement (Support2)	**Change of bending stress [%]**		
(mm)	**Support 1**	**Support 2**	**Support 3**
0	0,0%	0,0%	0,0%
1	0,0%	3,2%	0,0%
2	0,0%	6,3%	0,0%
20	0,0%	63,4%	0,0%

Bending moment and bending stress diagrams for kiln 3,4 m x 90 m when displacement is occurring at support 2 are shown in figure 34. The diagram shows bending moment and stress without axis misalignment, and with the displacements that increase support forces by 10%.

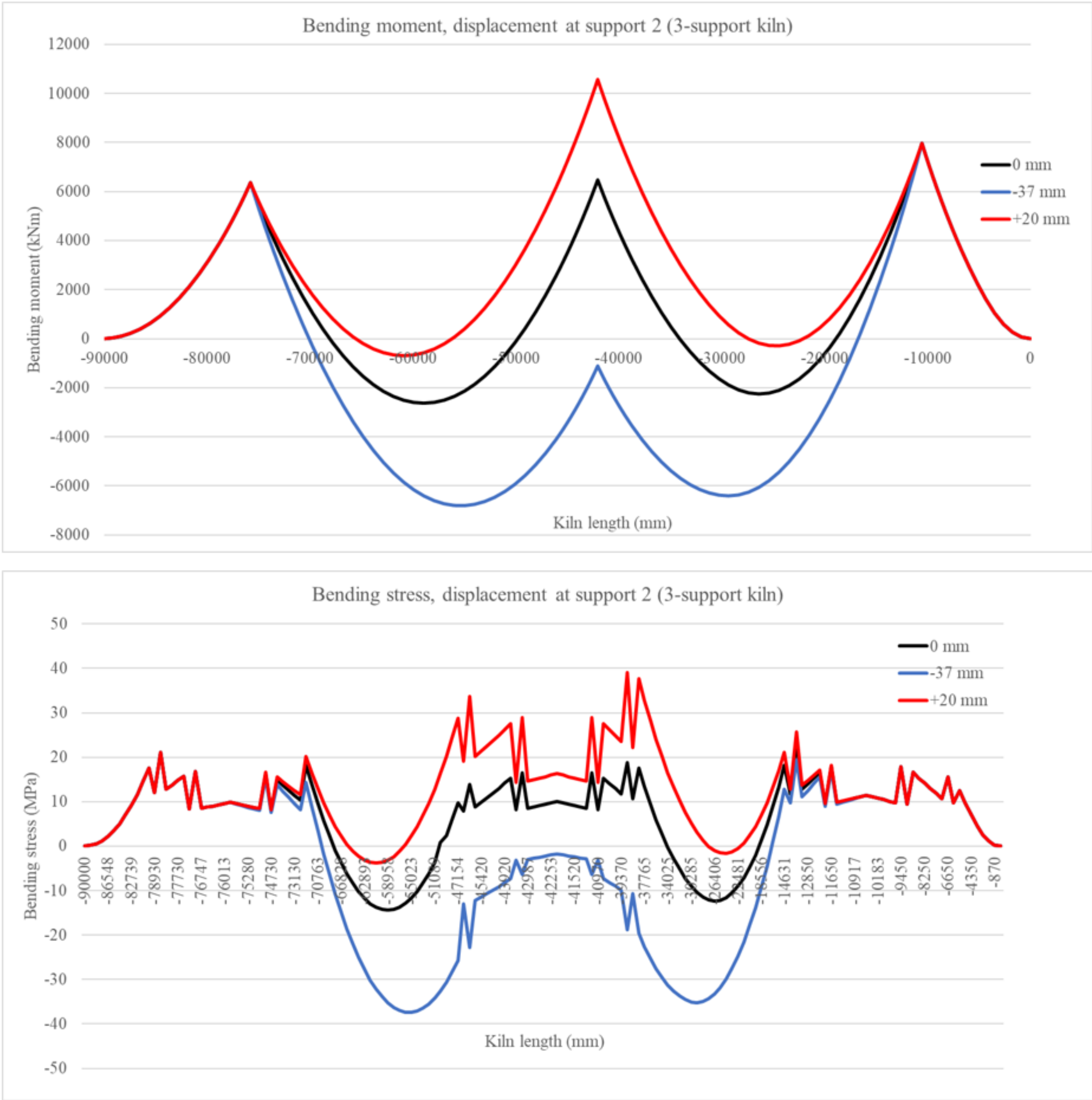

Figure 34. Bending moment and bending stress diagrams for kiln 3,4 m x 165 m, displacement at support 2.

8 DISCUSSION

In this chapter, discussion of the results of this thesis is conducted. First the main findings of literature review are presented. Then the functionality of the created 3D-model is analyzed. In addition, the effect of axis misalignment on support loads is discussed based on the results of the analyzes.

8.1 Literature findings

The literature review part of this thesis was divided into three different topics. Firstly, the overview of the process in chemical recovery and white liquor plant was described and the role of lime kiln as part of it. Also, the mechanical structure of the lime kiln was presented along with the topic as an introduction for the 3D-model creation phase. Based on the process description topic can be said that lime kiln is an important component as part of the chemical recovery and white liquor plant. Lime kiln allows to reuse the formed calcium carbonate again in the process by transforming it back to calcium oxide which is used for creation of white liquor.

Chapter three was dealing different damage that occurs while operating lime kiln. It was found that typically problems with shell are related to refractory lining damage that are exposing the shell to the heat. In turn, the refractory lining problems can be a reason for example overheating or increased ovality. Overall, constant monitoring of the kiln behavior is a key aspect for ensuring durable usage of lime kiln and predicting inevitable damage beforehand. For example, measuring and adjusting axis alignment is a way of increasing bearing life of support rollers. That is because axis misalignment state can be critical if it is affecting for a long period but can be corrected by adjustments. However, for example wearing occurs inevitably and for that reason maintenance procedures are needed at some point of the life of lime kiln. By regular measurements they can be predicted and that prevents them occurring suddenly.

Based on the third topic of literature review in chapter four, that was dealing top-down design process, was found that control of modification for 3D-models is more effective with top-down design than with traditional bottom-up method. When the components of the model are linked with each other, the modifications can be done uniformly, and it is effective way to create different versions of a structure for example. For that reason, the technique was used also at the experimental part of the thesis, where 3D-model for lime kiln shell section was made. In addition, theory of model-based definition was dealt. It means newer technique in design, where detailed information of the product is implemented into 3D-model, which reduces the need of 2D-drawings. Besides the challenges it is facing at the moment, it has potential for gaining popularity in the future.

8.2 Discussion of the functionality of lime kiln shell section 3D-model

The created 3D-model for lime kiln shell section design can be used for creating needed drawings as was mentioned in chapter 7.1. By the utilization of 3D-model the visual presentation of the designed structure has improved compared to for only having 2D-drawings. Besides that, the model is able to present the designed section along the length of the kiln which makes it more illustrative. The visual presentation of the structure could be also utilized for creation of images for different subdivisions. For example, when certain lime kiln shell section is offered to customer, in addition for the drawings, 3D-pictures could be offered for more illustrative view of the specific structure.

Compared to 2D-design process, the 3D-template model is able to reduce time that creation of the drawings consumes. For example, designing of section which included two shell plates, riding ring and filler bar structure, took 2,5 hours with the new 3D-model, when with 2D-desing, the needed time would be one to two days. The main difference comes with the automation of 3D-model, which creates projections and geometries automatically. With 2D-design, all the projections must be done manually which is time consuming work phase. Besides that, the changes of the structure can be implemented easier in 3D-model that 2D-drawings. For example, if the dimensions of the structure changes, the 3D-model configuration is possible to modify with ease by changing parameter values. That way the projections updates automatically, but with 2D-design, all the projections must be corrected manually. Also, when utilizing template model for design, the changes for example in design criteria or offered structures can be modified directly to the 0-model, when those changes are implemented concentratedly. That reduces the risk of design errors, specially if design is conducted by multiple persons. In general, one of the reasons for the automatization in design, is to minimize the risk of errors. The design could have been relied for certain expert or experts with high skill level, and if their contributions are disappearing, caused by retiring for example, similarly skilled persons may be difficult to find, and the quality of the design may drop.

However, for creating drawings in 3D-design, the model is always needed. That way in some cases, the 2D-design might be more flexible, because the creation of drawings could be started right away. Also, the development work of the template model requires resources and time, and training and maintenance when it is in use. That way, specially in the beginning of the usage of template model, the work may be more complex and rigid for high skill level personnel that are able to make the designing effectively in traditional way.

From the table 2 can be seen that the production of drawings is the most time-consuming phase of the usage of 3D-model. That is because the drawings weren't fully automated, and dimensioning and arrangement of the projections must be done manually. Although the lack of automation reduces the efficiency of the usage of created 3D-model, it is not totally bad thing. The manual work forces a designer to evaluate and think more that the dimensions and other features are correct and valid for the designed structure. For that reason, the fact that the drawings are not fully automated, may reduce dimensioning errors. Also, the nature of service work, or low volume production in general, the fully automated design processes are very difficult to develop, because of the high variation of the designed products. That way the balance between automation and manual work is important to find. The fully automated design process in more suitable for high volume production with less changing products.

8.3 Discussion of the effect of misalignment on support loads

The effect of misalignment for support loads is different based on the size of the kiln. From the chapter 7.2 can be seen that the support forces increased more with the five-support kiln than the three-support kiln when the misalignment was affected. The reason for that is combination of the effects of adjacent supports and the stiffness difference of the shell cross-sections. With three-support kiln, unsupported feed end and discharge end are affecting more compared to five-support kiln, which causes less resistance for the displacement. In addition, the stiffness of the cross-section increases when shell diameter is larger. Because of the stiffness, the 10% increase is reached with smaller displacements with the five-support kiln.

The most affects were caused by both kilns the scenario, where middle support is elevated. For the five-support kiln that causes 2,1% increase of the support force, and for three-support kiln 0,5% increase, when the displacement is 1 mm. That means the displacement causes about four times higher increase with five-support kiln than three-support kiln. The 10% limit of increase was then reached with five-support kiln at 5 mm displacement and with three-support kiln at 20 mm displacement. Based on the result can be said that the three-support is not that critical in terms of the support forces when misalignment is occurred. However, even if the increase of support forces is not as critical with three-support kiln that five-support kiln, larger misalignment can not be allowed. The axis misalignment causes other problems in addition to support forces, such as increase of power consumption and increase of wear, which is harmful for the shell, riding ring and refractory lining. For that reason, the kiln condition must be considered as a whole, rather than focusing on one particular value.

Along with the support forces, bending stress changes at the support locations were studied. For five-support kiln the changes follow the similar trend as with the support forces, however they were larger. With the most critical scenario, where displacement was at middle support for elevated direction, the bending stress increases 8,4% at 1 mm displacement and 42,0% when the displacement is 5 mm. Even if the bending stress increases more than the support forces, they are not considered more critical. The stresses are still not close to yield strengths, so they won’t cause sudden problem. However, if the increased state remains for a long period, it can be harmful. Increased stress levels caused increased ovality which means problems for the refractory. It also has an effect from the view of fatigue, which can be critical specially for the durability of attachment welds at the support locations if the fault state remains for a long time.

For the three-support kiln can be seen that if the support 1 elevates or support 2 sinks, the bending stresses at support locations doesn’t increase. That is because the bending stresses are moving towards the middle of the span and therefore reduces the stress at support locations. That can be verified also from the figure 34, where the bending stress diagram was shown along the length of the shell for the three-support kiln when displacement is occurring at support 2. When the displacement for downward direction increases, the bending stress at the sunken support decreases while the stress at middle of the span increases. The increase of the stress is notable, but in short term that is not considered as critical if any welds are not located at the area. If the welds are at the increased stress area, stress concentrations may occur, and they can be harmful. However, the 10% increase of support forces with three-support kiln is reached at high displacement values, which means there is probably other fault states occurred before the displacement is reached. That way the stress distribution shown in diagram may not be reached.

The results give good overview of the effect of misalignment on support forces. The phenomenon was tested with three-support and five-support kilns, which can be considered to give enough understanding of the topic. The five-support kiln can be considered to behave similarly as four-support and for that reason a four-support kiln was not under observation. Furthermore, the misalignment doesn’t affect on two-support kilns, and for that reason it wasn’t included to study. The misalignment was studied with scenarios that one support either is sunken or elevated. Naturally, that doesn’t include all the different phenomena that may occur, and probably the kiln does not experience exactly the situation that was tested. However, the test gives general understanding that the effect of misalignment is different with different sized kilns and if the misalignment occurs in different support for different direction. In addition, the values of change can be considered to be in similar range and following similar trend, even if the variations would be slightly different.

The analyzes can be considered reliable because the values of the support forces are similar range with other calculations that are made for dimensioning lime kilns. The beam-elements doesn’t describe local deformations of the cross-section, so some of the phenomena can not be observed with the model. Also, local deformation at contacts were not considered. There is flexibility at the contacts between riding rings and support rollers that causes local deformation, which means that the displacement of the support is not directly occurring at the centerline of the shell. However, the effect can be considered so small that it is not affecting to the results. In addition, static analyzes were made so the rotation of the shell was not implemented. That way for example ovality of the shell is not considered at the calculations which is important factor related to functionality of the shell. However, when studying more of a global effect, the beam model can be considered accurate and is enough for analyzing the problem. Also, the static analysis is enough for analyzing support reactions by that assumption that the shell is undeformed, and the so-called crank is not occurring.

That would require non-linear analysis where the rotation of the shell is considered. For the bending stresses the cross-sectional behavior is more relevant. That way at least with the small displacement values, the results of bending stresses are reliable. With high stresses the ovality for example might have been increased at the level where the stresses are changing locally in real structure and the beam element is not able to describe that.

9 CONCLUSIONS

The purpose of this thesis work was to develop parametric 3D-model that can be used for mechanical design related to maintenance project where section of lime kiln shell is replaced. In addition, axis misalignment, which is one of the fault states of the lime kiln was studied more closely and its effect on support loads were analyzed. The work was aiming to answer research questions that are presented next.

First question was “What are the main failure modes for the lime kiln that leads to section change repair work?”. The topic was dealt with literature review, where different fault states were presented. Many of the shell damage are related to refractory lining problems, that exposes the shell to the heat and causes deformations for instance. Refractory lining can be damaged because of increased ovality, which is a reason of excessive clearance between riding ring and shell that is caused by wearing. Based on the review can be noticed that lot of different problems are related to each other so basically everything affects everything. For that reason, it is important to regularly service the kiln and operate needed repair work, for ensuring proper functionality throughout the operating life of kiln.

Second question was “How parametric 3D-model could be utilized for efficient design of lime kiln shell section?”. The 3D-model was developed by top-down skeleton modelling which allows to create different configurations of the lime kiln shell section. The 3D-model is controlled by user interface in Excel environment. That way the user sets desired input parameters for the user interface, and the model generates wanted shell section design. The model is then used for creating manufacturing drawings for the designed structure. Follow-up question related to the 3D-model was “How the model affects on the efficiency of the design work of lime kiln shell section?”. Based on the test use of the model, it was able to decrease the time of design work of the shell section, even if the creation of drawings is not fully automated. With the 3D-model, drawing projections are generated automatically, when with 2D-desing they have to be created manually. Also, the modification of the structure is more flexible because the model updates automatically if parameters are changed. When also considering the visual presentation in 3D, ability to control the design guidelines centrally and the possible reduction of design errors, can be said that the parametric 3D-model is able to increase efficiency of the design process of lime kiln shell section.

Third research question was “What is the effect of kiln axis misalignment on support forces and bending stresses at support locations?” and follow-up question for it was “How the effect of axis misalignment on support loads differs with kilns with different sizes?”. The topic was analyzed by calculating support forces and bending stresses with different misalignment values for five-support and three-support kilns. Based on the results of the calculations can be said that the misalignment affects more on the support forces of five-support kiln than three-support kiln. The 10% increase of support forces was reached at 5 mm displacement of five-support kiln, when it was 20 mm with three-support kiln. The highest increase of support forces was occurring for both kilns when the middle support was elevated. Generally, support forces were increased at adjacent supports relative to support that was sunken and decreased when it was elevated. The change of bending stresses followed the same trend as with support forces with five-support kiln. However, with three-support kiln, there was scenarios where bending stresses were decreasing from supports and increasing at middle of spans. Overall, for the topic can be said that even with machines with hundreds of meters of length, few millimeters of misalignment can cause problems for the components. That emphasizes the meaning of measurements for the kiln axis, along with other service operations, in relation of durability of the kiln.

9.1 Further studies and future aspects

For the subject of further development of the parametric 3D-model could be creation of similar template model for the whole lime kiln shell. That way also the design of the new kilns could be transformed into 3D-environment. The created 3D-model could be used as a basis for the whole kiln shell template model. The user interface has database of the dimensions of standard kiln series, and it uses them as defaults dimensions for the structure. The skeleton structure could be expanded in a way that the master skeleton would define the whole shell and is divided into sub-skeletons that defines different shell sections at supports. Compared to shell section model, there is more components involved but the different possibilities for certain dimensions may reduce. For example, the section division of the shell is more stable and that way the location of site welded seams may be simpler to define. However, even though the dimensions of standard kiln series are determined, modifications may occur in the projects. That way the model needs to offer customizability like in the section model.

The effect of axis misalignment was studied in this work, and it gave more information about its effect on support forces and bending stresses. For further subject of study could be analyzing another fault state, deformation of the shell which causes shell crank, and its behavior along the length of shell. For estimating the behavior of the run-out caused by crank, cutting locations of the old shell could be determined when section change of the shell is executed. Also, installation tolerance for new section could be determined if the effect of run-out along the length of the shell is known. However, that might be difficult to assume by calculations, because the magnitude of the shell crank is related for many different factors, and specific generalizable guidelines could be hard to determine. Overall, increase of knowledge about the behavior of the shell crank and its effects could be useful information for understanding more deeply the functionality of lime kiln.

As was discussed about the importance of measurements of the lime kiln condition, new technologies can be assumed to be utilized for continuous condition monitoring in the future. For example, mechanical behavior of the kiln could be constantly measured with different sensors and measurement tools, and that way the disturbances could be noticed earlier. Along with the trend of digital transformation, in the future different digitalization tools such as digital twins could be implemented into lime kiln maintenance and that way be used for monitoring, and planning service operations efficiently.

10 SUMMARY

Lime kiln section change is a maintenance procedure where part of the old kiln shell is replaced with new one. The topic of this master's thesis was to develop parametric 3D-model as design tool lime kiln shell section design process which can be used for section change projects. In addition, effect of kiln axis misalignment on support loads was analyzed. Axis misalignment is fault state where kiln axis is not straight with respect different supports.

The thesis consists of two parts, literature review and practical development part. Literature review gave overview of the lime kiln structure and its function as part of a white liquor plant and chemical recovery. Also, different forms of damage that occur for the lime kiln during operation was presented. In addition, theory of the top-down design, skeleton modelling and introduce of model-state definition was part of the literature review. Practical part included development of parametric 3D-model for lime kiln shell section and study of the effect of axis misalignment of support loads.

The design tool for lime kiln shell section was developed by utilizing top-down skeleton modelling. Its purpose is to increase efficiency of the design process by creating different shell section configurations automatically and by enabling flexible modification of the designed structure. The model includes main components of the kiln shell that are shell plates, riding ring, filler bars and wear pieces. The template model is controlled by user interface. Based on the inputs on user interface, correct design is generated into 3D-model. Test usage of the model showed that the model can be utilized for designing of the lime kiln shell section, and it increases the efficiency of the design process even though creation of drawings is not fully automated. However, the 3D-model offers other improvements such as more illustrative presentation of product.

The effect of axis misalignment on support forces were tested with three-support and five-support kilns. Based on the results, support forces of five-support kiln were affected more by the misalignment. 5 mm of displacement value raised support force by 10 percent, which can be considered critical for durability of support roller bearings.

LIST OF REFERENCES

Andritz Oy. 2018. Operating and maintenance instruction: Support rollers. Recovery and Power, Kotka: Andritz Oy internal document. 42 p.

Andritz Oy. 2019. White liquor plant cross technology training. Recovery and Power, Internal document. 89 p.

Andritz Oy. 2020a. Operating and maintenance instruction: Lime kiln shell and riding rings. Recovery and Power, Kotka: Andritz Oy internal document. 23 p.

Andritz Oy, 2020b. Lime kiln shell and riding rings. Maintenance training. Recovery and power, Internal document. 17 p.

Andritz recovery and power. 2020. LimeKiln^{TM}. White liquor plant, Internal document. 48 p.

Autodesk. 2019. About iLogic Functionality. [web document]. [Referred 27.7.2021]. Available: https://knowledge.autodesk.com/support/inventor/learn-explore/caas/CloudHelp/cloudhelp/2020/ENU/Inventor-iLogic/files/GUID-9372F2A9-377E-40AB-92AA-5FC371BACF8C-htm.html

Autodesk. 2020. Why engineers design with parametric 3D. [web document]. [Referred 16.8.2021]. Autodesk, Inc. Available in PDF-file: https://damassets.autodesk.net/content/dam/autodesk/docs/pdfs/fy21-dm-pdmc-why-engineers-design-parametric-3D-en-asean.pdf.

Bajpai, P. 2016. Pulp and Paper Industry: Chemical Recovery. San Diego: Elsevier. 242 p.

Chen, X., Gao, S., Yang, Y. & Zhang, S. 2012. Multi-level assembly model for top-down design of mechanical products. Computer-Aided design, Vol. 44. pp. 1033-1048.

Chu, D., Lyu, G., Chu, X. & Shen, J. 2016. Multi-Skeleton model for top-down design of complex products. Advances in mechanical engineering, Vol. 8. pp. 1-20.

FLSmidth. 2015. Kiln services- Resurfacing of rollers and tyres, [web document] [Referred 20.7.2021]. FLSmidth. Available in PDF-file: https://flsmidth-prod-cdn.azureedge.net/-/media/brochures/brochures-services/operational-services/2000-2017/kiln-services---resurfacing-of-rollers-and-tyres.pdf?rev=6d14b307-dca2-45fa-b5ea-07d1965aff5b.

Gebhart, W. 1995. Rotating kiln tyres: lubricating between the tyre and shell. World cement, p. 4.

Hobbacher, A. 2008. Recommendations for fatigue design of welded joints and components. Paris: International Institute of welding. 149 p.

Janati, K. 2020. Thermo-elastic behavior study of rotary kilns for cement plants. Engineering Failure Analysis, Vol. 118. pp. 1-13.

Jiao, L. L. 2014. Design of Valve Parametric Variant Template Based on NX. Applied mechanics and materials, Vol. 697. pp. 289-292.

KnowPulp, 2021. KnowPulp 19.0 -learning environment. [web document]. [Referred 2.3.2021]. Service is chargeable and needs user license.

Koskinen, T. & Mussalo, M. 2006. Meesauunin mekaaninen mitoitus ja komponentit. Chemical systems division, Kotka: Andritz Oy internal document. 64 pp.

Nguyen, J. 2021. MBD (Model-Based Definition): 2021 Edition. [web document]. [Referred 4.8.2021]. Available at: https://www.capvidia.com/blog/mbd-model-based-definition-in-the-21st-century

Pere, A. 2016. Koneenpiirustus 1&2. 12th edition. Espoo: Kirpe Oy. 811 p.

Quintana, V., Rivest, L., Pellerin, R., Venne, F. & Kheddouci, F. 2010. Will Model-based Definition replace engineering drawings throughout the product lifecycle? A global perspective from aerospace industry. Computers in industry, Vol. 61. pp. 497-508.

Sengupta, P. 2020. Refractories for the Chemical Industries. Cham: Springer. 377 p.

SFS-EN 1993-1-9. 2008. Eurocode 3: Design of steel structures. Part 1-9: Fatigue, Helsinki: Suomen Standardisoimisliitto SFS. 41 p. Confirmed and published in English.

Theliander, H. 2009. The Recovery of cooking chemicals: The white liquor preparation plant. In: Pulping Chemistry and Technology. Berlin: De Gruyter. pp. 335-362.

Thilo, M. 2019. What is the future of technical drawings? [web document]. [Referred 2.8.2021]. Available at: https://knowledge.autodesk.com/support/inventor/getting-started/caas/simplecontent/content/what-the-future-technical-drawings.html

TomTom-Tools GmbH, 2018a. User Manual: OVALITY SENSOR II, Arni: TomTom-Tools GmbH. 16 p.

Tom-Tom Tools GmbH 2018b. User Manual: Inductive Distance Measurement (IDM) Tool Kit, Arni: Tom-Tom Tools GmbH. 28 p.

TomTom-Tools GmbH, 2018c. User manual: Kiln Axis Alignment System. Arni: TomTom-Tools GmbH. 20 p.

Varitis, E., Rinos, K. & Kostis, N. 2020. Model-based definition capabilities and its impact on industrial productivity. MATEC web of conferences, Vol. 318. pp. 1-6.

Wisner, A., 2020. Top 5 critical maintenance issues for rotary kilns. [web document]. [Referred 19.7.2021]. Available at: https://www.mogroup.com/insights/blog/mining-and-metals/top-5-critical-maintenance-issues-for-rotary-kilns/

Yougang, X., Xuejun, L. & Xiaoqing, C. 2008. General solution to kiln support reactions and multi-objective fuzzy optimization of kiln axis alignment. Structural and multidisciplinary optimization, Vol. 36. pp. 319-327.

Model user interface, input data sheet

LimeKiln shell 3D-model - User Input Data

Set desired settings and parameters.

Kiln data general

	Default Value (Select Value)		Edit Value	
Type	LK45125_Gas			Select the Kiln type
Incline	2,5	%		Incline of the kiln
Shell_ID	4500	mm		Inside diameter of the shell
Kiln_length	125000	mm		Length of the kiln

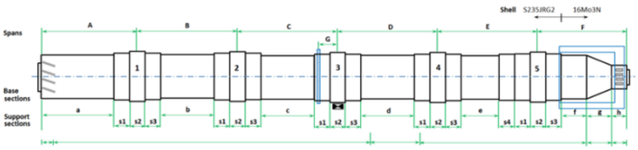

(Check the span lengths from reference kiln information)

Section data

	Default Value		Edit Value	
Selection of support for change	Support2			Select which support/pier the kiln section is located
Support2_Hot_End_Distance	3000	mm	3000	(If non standard, copy from reference kiln data)

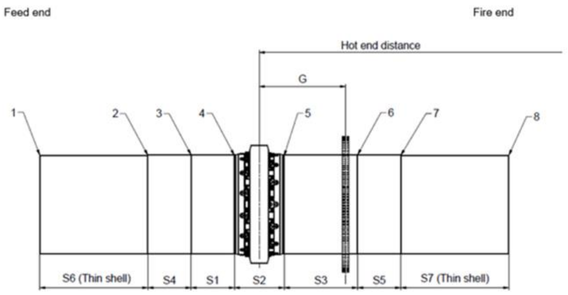

Select active shell parts

Select seam types ("Site" includes clamps)

S6_active	S4_active	S1_active	S2_active	S3_active	S5_active	S7_active
Yes	No	Yes	Yes	Yes	No	Yes

Seam 1	Seam 2	Seam 3	Seam 4	Seam 5	Seam 6	Seam 7	Seam 8
Site	Site	Workshop	Workshop	Workshop	Workshop	Site	Site

Riding_Ring_Active	Riding_Ring_Type	Filler bars	Clamp_Type
Yes	Guiding	No	M52

Kiln information (Reference)

	Default Value		Edit Value
Number of supports	5		
Span_A_Length	1000	mm	1000
Span_B_Length	1000	mm	1000
Span_C_Length	1000	mm	1000
Span_D_Length	1000	mm	1000
Span_E_Length	1000	mm	1000
Span_F_Length	0	mm	
Support1_Hot_End_Distance	4000	mm	
Support2_Hot_End_Distance	3000	mm	
Support3_Hot_End_Distance	2000	mm	
Support4_Hot_End_Distance	1000	mm	
Support5_Hot_End_Distance	0	mm	
Kiln_length_Non_Standard	5000		

	Default Value		Edit Value	
Girth_Ring	Yes			Select does the reference kiln include girth ring
Girth_Ring_Position	Downhill			Select which side of the drive pier girth ring locates
Girth_Ring_Distance (G)	1000	mm	1000	Distance from drive pier
Girth_Ring_OD	1000	mm	1000	Outside diameter of girth ring
Girth_Ring_Width	1000	mm	1000	Width of the girth ring
Girth_Ring_Tooth_Number	100	pcs	100	Tooth number of the girth ring

Ring data

Support2_Ring_OD	1000	mm	1000	Outside diameter of the ring
Support2_Ring_ID	1000	mm	1000	Inside diameter of the ring
Support2_Ring_Face_Width	1000	mm	1000	Ring width (at the outside diameter)
Support2_Guiding_Ring_Contact_Angle	99	deg	99	Contact angle of the guiding ring (select 0 if the guiding ring is not selected
Support2_Guiding_Ring_Contact_Height	99	mm	99	Contact height of the guiding ring
Support2_Guiding_Ring_Total_Width	99	mm	99	Total width of the ring (If regular ring total width is the same as face width)
Radial_Clearance	-3896	mm		

Filler bar data

(Details must be determined in the model)

Filler_Bar_Width	99	mm	99	Filler bar width
Filler_Bar_Length	99	mm	99	Filler bar length
Filler_Bar_Thickness	99	mm	99	Filler bar thickness
Filler_Bar_Number	99		99	Number of filler bars

S6 data (Thin shell)

S6_Thickness	99	mm	99	Thin shell thickness at uphill side of support
S6_Length	99	mm	99	Thin shell width at uphill side of support
Distance_From_Support2_S6	99		99	Distance of the thin shell at support

S7 data (Thin shell)

S7_Thickness	99	mm	99	Thin shell thickness at downhill side of support
S7_Lenght	99	mm	99	Thin shell width at downhill side of support
Distance_From_Support2_S7	49,5			Distance of the thin shell at support

Wear piece data

Wear_Piece_Number	99	pcs	99	Number of wear pieces (without filler bar)
Wear_Piece_Height	60	mm	99	Height of the wear piece

Clamps

Clamp_Number	99	pcs	99	Number of connecting devices

Shell Offset

Shell_Offset	99	mm	99	Shell offset related to riding ring. If the wanted offset is at downhill side, offset value must be neagtive

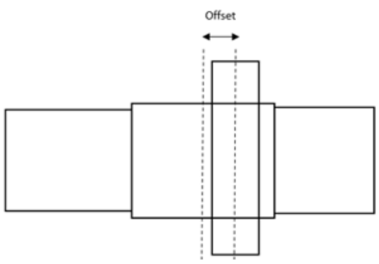

S4 Data

Support2_S4_Thickness	35	mm	35	S4 plate thickness (if not active select 99 mm)
Support2_S4_Length	99	mm	99	S4 plate length (if not active select 99 mm)

S2 Data (Heavy shell)

Support2_S2_Thickness	99	mm	99	S2 plate (heavyshell) thickness
Support2_S2_Length	99	mm	99	S2 plate (heavyshell) length

S1 Data

Support2_S1_Thickness	99	mm	99	S1 plate thickness (check correct value even if S1 is not active)
Support2_S1_Length	99	mm	99	S1 plate length

S3 Data

Support2_S3_Thickness	99	mm	99	S3 plate thickness (check correct value even if S3 is not active)
Support2_S3_Length	99	mm	99	S3 plate length

S5 Data

Support2_S5_Thickness	99	mm	99	S5 plate thickness (if not active select 99 mm)
Support2_S5_Length	99	mm	99	S5 plate length (if not active select 99 mm)

Result set for kiln 5,5 m x 165 m

Displacement (Support2)	**Change of support force [%]**				
(mm)	**Support1**	**Support2**	**Support3**	**Support4**	**Support5**
0	0,00 %	0,00 %	0,00 %	0,00 %	0,00 %
-1	0,64 %	-1,63 %	1,47 %	-0,54 %	0,07 %
-2	1,27 %	-3,27 %	2,94 %	-1,08 %	0,14 %
-3	1,91 %	-4,90 %	4,41 %	-1,62 %	0,22 %
-4	2,54 %	-6,53 %	5,88 %	-2,15 %	0,29 %
-5	3,18 %	-8,16 %	7,35 %	-2,69 %	0,36 %
-6	3,81 %	-9,80 %	8,82 %	-3,23 %	0,43 %
-7	4,45 %	-11,43 %	10,29 %	-3,77 %	0,51 %
-8	5,09 %	-13,06 %	11,76 %	-4,31 %	0,58 %
-9	5,72 %	-14,70 %	13,23 %	-4,85 %	0,65 %
-10	6,36 %	-16,33 %	14,70 %	-5,39 %	0,72 %
-11	6,99 %	-17,96 %	16,17 %	-5,93 %	0,80 %
-12	7,63 %	-19,59 %	17,64 %	-6,46 %	0,87 %
-13	8,26 %	-21,23 %	19,11 %	-7,00 %	0,94 %

Displacement (Support2)	**Change of support force [%]**				
(mm)	**Support1**	**Support2**	**Support3**	**Support4**	**Support5**
0	0,00 %	0,00 %	0,00 %	0,00 %	0,00 %
1	-0,63 %	1,63 %	-1,47 %	0,54 %	-0,07 %
2	-1,27 %	3,26 %	-2,94 %	1,08 %	-0,15 %
3	-1,91 %	4,90 %	-4,41 %	1,62 %	-0,22 %
4	-2,54 %	6,53 %	-5,88 %	2,16 %	-0,29 %
5	-3,18 %	8,16 %	-7,35 %	2,69 %	-0,36 %
6	-3,81 %	9,80 %	-8,82 %	3,23 %	-0,43 %
7	-4,45 %	11,43 %	-10,29 %	3,77 %	-0,51 %
8	-5,08 %	13,06 %	-11,76 %	4,31 %	-0,58 %
9	-5,72 %	14,69 %	-13,23 %	4,85 %	-0,65 %
10	-6,35 %	16,33 %	-14,70 %	5,39 %	-0,72 %
11	-6,99 %	17,96 %	-16,17 %	5,93 %	-0,80 %
12	-7,63 %	19,59 %	-17,64 %	6,47 %	-0,87 %
13	-8,26 %	21,23 %	-19,11 %	7,01 %	-0,94 %

Displacement (Support3)	Change of support force [%]				
(mm)	Support1	Support2	Support3	Support4	Support5
0	0,00 %	0,00 %	0,00 %	0,00 %	0,00 %
-1	-0,45 %	1,55 %	-2,09 %	1,28 %	-0,28 %
-2	-0,89 %	3,10 %	-4,19 %	2,55 %	-0,55 %
-3	-1,34 %	4,65 %	-6,28 %	3,82 %	-0,83 %
-4	-1,79 %	6,20 %	-8,38 %	5,10 %	-1,10 %
-5	-2,24 %	7,75 %	-10,47 %	6,37 %	-1,38 %
-6	-2,69 %	9,30 %	-12,57 %	7,65 %	-1,65 %
-7	-3,14 %	10,85 %	-14,66 %	8,92 %	-1,93 %
-8	-3,58 %	12,41 %	-16,76 %	10,20 %	-2,20 %
-9	-4,03 %	13,96 %	-18,85 %	11,47 %	-2,48 %
-10	-4,48 %	15,51 %	-20,94 %	12,75 %	-2,76 %
-11	-4,93 %	17,06 %	-23,04 %	14,02 %	-3,03 %
-12	-5,37 %	18,61 %	-25,13 %	15,30 %	-3,31 %
-13	-5,82 %	20,16 %	-27,23 %	16,57 %	-3,58 %

Displacement (Support3)	Change of support force [%]				
(mm)	Support1	Support2	Support3	Support4	Support5
0	0,00 %	0,00 %	0,00 %	0,00 %	0,00 %
1	0,45 %	-1,55 %	2,09 %	-1,27 %	0,28 %
2	0,90 %	-3,10 %	4,19 %	-2,55 %	0,55 %
3	1,35 %	-4,65 %	6,28 %	-3,82 %	0,83 %
4	1,79 %	-6,20 %	8,38 %	-5,10 %	1,10 %
5	2,24 %	-7,75 %	10,47 %	-6,37 %	1,38 %
6	2,69 %	-9,30 %	12,57 %	-7,65 %	1,65 %
7	3,14 %	-10,86 %	14,66 %	-8,92 %	1,93 %
8	3,58 %	-12,41 %	16,76 %	-10,20 %	2,20 %
9	4,03 %	-13,96 %	18,85 %	-11,47 %	2,48 %
10	4,48 %	-15,51 %	20,95 %	-12,75 %	2,76 %
11	4,93 %	-17,06 %	23,04 %	-14,02 %	3,03 %
12	5,38 %	-18,61 %	25,13 %	-15,30 %	3,31 %
13	5,82 %	-20,16 %	27,23 %	-16,57 %	3,58 %

Displacement (Support2)	Change of bending stress [%]				
(mm)	Support1	Support2	Support3	Support4	Support5
0	0,00 %	0,00 %	0,00 %	0,00 %	0,00 %
-1	0,00 %	-7,75 %	5,12 %	-1,22 %	0,00 %
-2	0,00 %	-15,49 %	10,23 %	-2,43 %	0,00 %
-3	0,00 %	-23,23 %	15,35 %	-3,65 %	0,00 %
-4	0,00 %	-30,98 %	20,46 %	-4,86 %	0,00 %
-5	0,00 %	-38,72 %	25,58 %	-6,08 %	0,00 %
-6	0,00 %	-46,47 %	30,69 %	-7,29 %	0,00 %
-7	0,00 %	-54,21 %	35,81 %	-8,51 %	0,00 %
-8	0,00 %	-61,96 %	40,93 %	-9,72 %	0,00 %
-9	0,00 %	-69,70 %	46,04 %	-10,94 %	0,00 %
-10	0,00 %	-77,45 %	51,15 %	-12,15 %	0,00 %
-11	0,00 %	-85,19 %	56,26 %	-13,37 %	0,00 %
-12	0,00 %	-92,93 %	61,38 %	-14,59 %	0,00 %
-13	0,00 %	-99,32 %	66,50 %	-15,80 %	0,00 %

Displacement (Support2)	Change of bending stress [%]				
(mm)	Support1	Support2	Support3	Support4	Support5
0	0,00 %	0,00 %	0,00 %	0,00 %	0,00 %
1	0,00 %	7,74 %	-5,12 %	1,21 %	0,00 %
2	0,00 %	15,49 %	-10,23 %	2,43 %	0,00 %
3	0,00 %	23,23 %	-15,35 %	3,65 %	0,00 %
4	0,00 %	30,98 %	-20,46 %	4,86 %	0,00 %
5	0,00 %	38,72 %	-25,58 %	6,08 %	0,00 %
6	0,00 %	46,47 %	-30,69 %	7,29 %	0,00 %
7	0,00 %	54,22 %	-35,81 %	8,51 %	0,00 %
8	0,00 %	61,95 %	-40,92 %	9,72 %	0,00 %
9	0,00 %	69,69 %	-46,04 %	10,94 %	0,00 %
10	0,00 %	77,44 %	-51,15 %	12,15 %	0,00 %
11	0,00 %	85,19 %	-56,27 %	13,37 %	0,00 %
12	0,00 %	92,93 %	-61,38 %	14,58 %	0,00 %
13	0,00 %	100,68 %	-66,50 %	15,80 %	0,00 %

Displacement (Support3)	Change of bending stress [%]				
(mm)	Support1	Support2	Support3	Support4	Support5
0	0,00 %	0,00 %	0,00 %	0,00 %	0,00 %
-1	0,00 %	5,46 %	-8,40 %	4,63 %	0,00 %
-2	0,00 %	10,92 %	-16,79 %	9,26 %	0,00 %
-3	0,00 %	16,38 %	-25,19 %	13,89 %	0,00 %
-4	0,00 %	21,84 %	-33,59 %	18,52 %	0,00 %
-5	0,00 %	27,29 %	-41,98 %	23,16 %	0,00 %
-6	0,00 %	32,75 %	-50,38 %	27,79 %	0,00 %
-7	0,00 %	38,21 %	-58,78 %	32,42 %	0,00 %
-8	0,00 %	43,67 %	-67,18 %	37,05 %	0,00 %
-9	0,00 %	49,13 %	-75,57 %	41,68 %	0,00 %
-10	0,00 %	54,59 %	-83,97 %	46,31 %	0,00 %
-11	0,00 %	60,05 %	-92,37 %	50,94 %	0,00 %
-12	0,00 %	65,51 %	-99,24 %	55,58 %	0,00 %
-13	0,00 %	70,97 %	-90,84 %	60,20 %	0,00 %

Displacement (Support3)	Change of bending stress [%]				
(mm)	Support1	Support2	Support3	Support4	Support5
0	0,00 %	0,00 %	0,00 %	0,00 %	0,00 %
1	0,00 %	-5,46 %	8,40 %	-4,63 %	0,00 %
2	0,00 %	-10,92 %	16,79 %	-9,26 %	0,00 %
3	0,00 %	-16,38 %	25,19 %	-13,89 %	0,00 %
4	0,00 %	-21,84 %	33,59 %	-18,53 %	0,00 %
5	0,00 %	-27,30 %	41,98 %	-23,16 %	0,00 %
6	0,00 %	-32,75 %	50,38 %	-27,79 %	0,00 %
7	0,00 %	-38,21 %	58,78 %	-32,42 %	0,00 %
8	0,00 %	-43,67 %	67,18 %	-37,05 %	0,00 %
9	0,00 %	-49,13 %	75,57 %	-41,68 %	0,00 %
10	0,00 %	-54,59 %	83,97 %	-46,31 %	0,00 %
11	0,00 %	-60,05 %	92,37 %	-50,94 %	0,00 %
12	0,00 %	-65,51 %	100,76 %	-55,57 %	0,00 %
13	0,00 %	-70,97 %	109,16 %	-60,20 %	0,00 %

Result set for kiln 3,4 m x 90 m

Displacement (Support1)	Change of support force [%]		
(mm)	Support 1	Support 2	Support 3
0	0,00 %	0,00 %	0,00 %
-1	-0,13 %	0,25 %	-0,11 %
-2	-0,26 %	0,50 %	-0,22 %
-3	-0,40 %	0,75 %	-0,33 %
-4	-0,53 %	1,00 %	-0,44 %
-5	-0,66 %	1,25 %	-0,54 %
-6	-0,79 %	1,50 %	-0,66 %
-7	-0,92 %	1,75 %	-0,76 %
-8	-1,06 %	2,00 %	-0,87 %
-9	-1,19 %	2,25 %	-0,98 %
-10	-1,32 %	2,50 %	-1,09 %
-40	-5,29 %	10,00 %	-4,36 %

Displacement (Support1)	Change of support force [%]		
(mm)	Support 1	Support 2	Support 3
0	0,00 %	0,00 %	0,00 %
1	0,14 %	-0,25 %	0,11 %
2	0,27 %	-0,50 %	0,22 %
3	0,40 %	-0,75 %	0,33 %
4	0,53 %	-1,00 %	0,44 %
5	0,66 %	-1,25 %	0,54 %
6	0,80 %	-1,50 %	0,66 %
7	0,93 %	-1,75 %	0,76 %
8	1,06 %	-2,00 %	0,87 %
9	1,19 %	-2,25 %	0,98 %
10	1,33 %	-2,50 %	1,09 %
75	9,93 %	-18,75 %	8,17 %
76	10,06 %	-19,00 %	8,28 %

Displacement (Support2)	Change of support force [%]		
(mm)	Support 1	Support 2	Support 3
0	0,00 %	0,00 %	0,00 %
-1	0,28 %	-0,52 %	0,23 %
-2	0,55 %	-1,04 %	0,45 %
-3	0,83 %	-1,55 %	0,68 %
-4	1,10 %	-2,07 %	0,90 %
-5	1,37 %	-2,59 %	1,13 %
-6	1,65 %	-3,11 %	1,36 %
-7	1,92 %	-3,62 %	1,58 %
-8	2,20 %	-4,14 %	1,81 %
-9	2,47 %	-4,66 %	2,03 %
-10	2,74 %	-5,18 %	2,26 %
-35	9,60 %	-18,12 %	7,90 %
-36	9,87 %	-18,64 %	8,12 %
-37	10,15 %	-19,16 %	8,35 %

Displacement (Support2)	Change of support force [%]		
(mm)	Support 1	Support 2	Support 3
0	0,00 %	0,00 %	0,00 %
1	-0,27 %	0,52 %	-0,23 %
2	-0,55 %	1,04 %	-0,45 %
3	-0,82 %	1,55 %	-0,68 %
4	-1,10 %	2,07 %	-0,90 %
5	-1,37 %	2,59 %	-1,13 %
6	-1,64 %	3,11 %	-1,36 %
7	-1,92 %	3,62 %	-1,58 %
8	-2,19 %	4,14 %	-1,81 %
9	-2,47 %	4,66 %	-2,03 %
10	-2,74 %	5,18 %	-2,26 %
20	-5,48 %	10,36 %	-4,51 %

Displacement (Support1)	Change of bending stress [%]		
(mm)	Support 1	Support 2	Support 3
0	0,00 %	0,00 %	0,00 %
-1	0,00 %	1,53 %	0,00 %
-2	0,00 %	3,06 %	0,00 %
-3	0,00 %	4,59 %	0,00 %
-4	0,00 %	6,12 %	0,00 %
-5	0,00 %	7,65 %	0,00 %
-6	0,00 %	9,18 %	0,00 %
-7	0,00 %	10,70 %	0,00 %
-8	0,00 %	12,23 %	0,00 %
-9	0,00 %	13,76 %	0,00 %
-10	0,00 %	15,29 %	0,00 %
-40	0,00 %	61,19 %	0,00 %

Displacement (Support1)	Change of bending stress [%]		
(mm)	Support 1	Support 2	Support 3
0	0,00 %	0,00 %	0,00 %
1	0,00 %	-1,53 %	0,00 %
2	0,00 %	-3,06 %	0,00 %
3	0,00 %	-4,59 %	0,00 %
4	0,00 %	-6,12 %	0,00 %
5	0,00 %	-7,65 %	0,00 %
6	0,00 %	-9,18 %	0,00 %
7	0,00 %	-10,71 %	0,00 %
8	0,00 %	-12,24 %	0,00 %
9	0,00 %	-13,77 %	0,00 %
10	0,00 %	-15,30 %	0,00 %
75	0,00 %	-114,73 %	0,00 %
76	0,00 %	-116,26 %	0,00 %

Displacement (Support2)	Change of bending stress [%]		
(mm)	Support 1	Support 2	Support 3
0	0,00 %	0,00 %	0,00 %
-1	0,00 %	-3,17 %	0,00 %
-2	0,00 %	-6,34 %	0,00 %
-3	0,00 %	-9,51 %	0,00 %
-4	0,00 %	-12,67 %	0,00 %
-5	0,00 %	-15,84 %	0,00 %
-6	0,00 %	-19,01 %	0,00 %
-7	0,00 %	-22,18 %	0,00 %
-8	0,00 %	-25,35 %	0,00 %
-9	0,00 %	-28,51 %	0,00 %
-10	0,00 %	-31,68 %	0,00 %
-35	0,00 %	-110,89 %	0,00 %
-36	0,00 %	-114,06 %	0,00 %
-37	0,00 %	-117,23 %	0,00 %

Displacement (Support2)	Change of bending stress [%]		
(mm)	Support 1	Support 2	Support 3
0	0,00 %	0,00 %	0,00 %
1	0,00 %	3,17 %	0,00 %
2	0,00 %	6,33 %	0,00 %
3	0,00 %	9,50 %	0,00 %
4	0,00 %	12,67 %	0,00 %
5	0,00 %	15,84 %	0,00 %
6	0,00 %	19,01 %	0,00 %
7	0,00 %	22,17 %	0,00 %
8	0,00 %	25,35 %	0,00 %
9	0,00 %	28,52 %	0,00 %
10	0,00 %	31,69 %	0,00 %
20	0,00 %	63,36 %	0,00 %